Research Square

Preprints are preliminary reports that have not undergone peer review.
They should not be considered conclusive, used to inform clinical practice,
or referenced by the media as validated information.

Fabrication and Optimization of Sesamol-Loaded Nanoemulgel for Skin Cancer: Insights from Molecular Modeling, In Vitro and In Vivo Studies

Vinod Kumar
vksingh38@yahoo.com
GD Goenka University
Manisha Singh
GD Goenka University
Manish Yadav
GD Goenka University
Aman Thakur
Shobhit University
Swati Kaushik
K.R. Mangalam University
Susmita Yadav
K.R. Mangalam University
Kirti Sharma
Saraswati Institute of Pharmaceutical Education and Research, SGC Group

Research Article

Keywords: Skin Cancer, Sesamol, Nanoemulgels, cytotoxicity studies, In Silico studies, Topical Drug Delivery

Posted Date: July 31st, 2026

DOI: https://doi.org/10.21203/rs.3.rs-10364673/v1

License: This work is licensed under a Creative Commons Attribution 4.0 International License.
Read Full License

Additional Declarations: No competing interests reported.

Title Page

Fabrication and Optimization of Sesamol-Loaded Nanoemulgel for Skin Cancer: Insights from Molecular Modeling, *In Vitro and In Vivo* Studies

Manisha Singh[1], Manish Yadav[1], Aman Thakur[2], Swati Kaushik[3], Susmita Yadav[3] , Kirti Sharma[4], Vinod Kumar[1] *

[1]School of Healthcare & Allied Sciences, G D Goenka University, Sohna Road Gurugram, Haryana 122103, India
[2]Adarsh Vijendra Institute of Pharmaceutical Sciences, Shobhit University, Gangoh, Saharanpur, Uttar Pradesh 247341, India
[3]School of Medical and Allied Sciences, K.R. Mangalam University, Sohna Road Gurugram, Haryana 122103, India
[4] Saraswati Institute of Pharmaceutical Education and Research, SGC Group, Gharuan-140413, Mohali, Punjab, India

***Corresponding Author**
Dr Vinod Kumar
Department of Pharmacy, G.D. Goenka University, Sohna Road, Gurugram-122103
Email: vksingh38@yahoo.com
Orcid ID: 0000-0002-4617-8037

*Corresponding author

Prof. Dr. Vinod Kumar

Department of Pharmacy, G.D. Goenka University, Sohna Road, Gurugram-122103

E-mail: vksingh38@yahoo.com

Authors' contributions

Conceptualization: Dr Vinod Kumar and Dr Manish Yadav; **Methodology:** Ms Manisha Singh; **Formal analysis and investigation:** Ms Manisha Singh, Mr Aman Thakur; **Writing - original draft preparation:** Ms Manisha Singh and Dr Swati Kaushik; **Writing - review and editing:** Dr Kirti Sharma and Dr Susmita Kumari Yadav; **Resources:** Dr Vinod Kumar; **Supervision:** Dr Vinod Kumar

Ethics Approval

This study was being approved for the animal experimentation, and the approval was taken from the IAEC of Deshpandey Laboratories, Bhopal (CPCSEA no. 1582/PO/Research/5/11/CPCSEA).

Competing Interests

The authors declare no competing interests.

Acknowledgement

We are thankful to SAIF, Guru Jambheshwar University, Hissar, for providing instrumentation facility to completion of the research work.

Data availability statement

The supplementary data will be made available on request.

Fabrication and Optimization of Sesamol-loaded Nanoemulgels for Skin Cancer: Insights from Molecular Modeling, *In Vitro and In Vivo* Studies

Manisha Singh[1], Manish Yadav[1], Aman Thakur[2], Swati Kaushik[3], Susmita Yadav[3] , Kirti Sharma[4] , Vinod Kumar[1] *

[1]School of Healthcare & Allied Sciences, G D Goenka University, Sohna Road Gurugram, Haryana 122103, India

[2]Adarsh Vijendra Institute of Pharmaceutical Sciences, Shobhit University, Gangoh, Saharanpur, Uttar Pradesh 247341, India

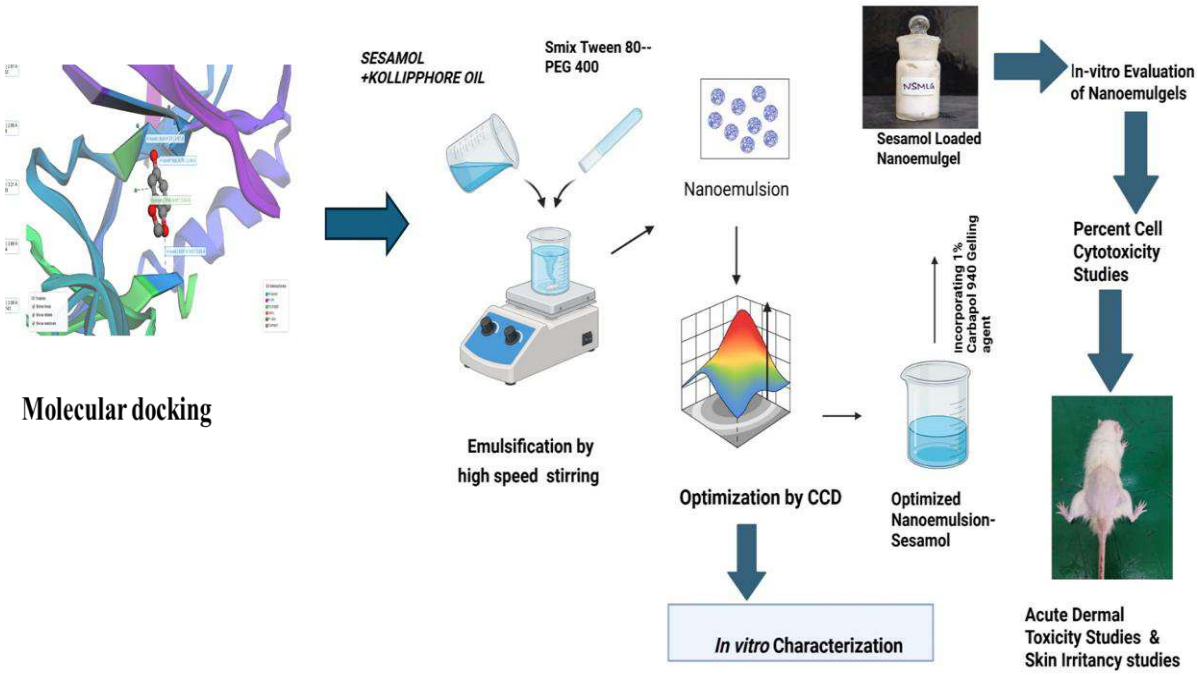
[3]School of Medical and Allied Sciences, K.R. Mangalam University, Sohna Road Gurugram, Haryana 122103, India

[4] Saraswati Institute of Pharmaceutical Education and Research, SGC Group, Gharuan-140413, Mohali, Punjab, India

*Address correspondence to this author at the Department of Pharmacy, G.D. Goenka University, Sohna Road, Gurugram-122103

Email: vksingh38@yahoo.com

Graphical Abstract



Abstract

Purpose

The current investigation aimed to develop nanoemulgel based topical delivery system for Sesamol (SES) and evaluate its therapeutic efficacy against skin cancer supported by in silico ADME profiling, molecular modeling,in vitro and in vivo assessments.

Methods

The human BRAF serine/threonine-protein kinase is a key component of the MAPK signaling pathway implicated in melanoma progression. To explore the probable binding of SES with this enzyme molecular docking studies were performed. SES's pharmacokinetic/toxicity profile was predicted via PharmoADMET using its SMILES structure. SES loaded nanoemulsions (SES-NE) was made by aqueous titration, optimized with a Central Composite Design, subsequently formulated into Carbopol based SES-nanoemulgel (SES-NEG) and evaluated for physicochemical properties, A375-melanoma cytotoxicity, dermal toxicity, and skin irritation in Wistar rats.

Results

Molecular docking studies of SES exhibited strong binding affinity of -10.7 kcal/mol by interacting with crucial residues Asp143 & Thr81 of BRAF followed by Pharmoscore of 90/100 explaining good prediction confidence and excellent ADMET profile of candidate. Optimized SES-NE produced globules averaging 215 ± 1.3 nm in size, a polydispersity index of 0.273 ± 0.013, a zeta potential of −22 ± 0.016 mV, and an entrapment efficiency of 81.8 ± 0.52%. SES-NEG exhibited suitable pH (5.9 ± 0.024), viscosity (257.97 ± 12.32 cps), and spreadibility (28.17 ± 0.015 g·cm/s) for topical application. SES-NEG exhibited significantly higher cytotoxicity against A375-melanoma cells compared to pristine SES with an IC_{50} of 23.21 ± 0.09 µg/mL, while exhibiting no systemic toxicity or irritation.

Conclusion

The optimistic results of the current study showed that SES-NEG is a safe, stable, and effective topical delivery system that significantly enhances anticancer efficacy, making it a potential approach for topical delivery in the management of skin carcinoma.

Keywords: Skin Cancer, Sesamol, Nanoemulgels, *cytotoxicity studies*, *In Silico* studies, Topical Drug Delivery

INTRODUCTION

Skin cancer is a major global public health issue, and the incidence rate has seen an alarming rise worldwide over the past decade. As per GLOBOCAN 2022 an approximate 331,722 incidence of skin melanomas and 1.20 million occurrences of non-melanoma skin canc were reported in the year 2022. This is equivalent to 43% of all cancers diagnosed worldwide [1,2].

Although the occurrence of skin cancer in India is low in proportion to all other cancers in India and other regions of the world, the incidence of skin cancer in India has been rising over the past decade. The Indian Council of Medical Research (ICMR), reported in 2022 that the estimated number of incident occurrence of skin carcinoma in India for 2022 was 1,461,427 [3]. Nonmelanoma skin cancer (NMSC) is the commonest skin cancer diagnosed in the Indian population, which accounts for 95% of all skin carcinoma, and skin melanomas makes for about 5% of all skin carcinoma cases [4].

Consequently, skin cancer is a serious condition of global health that has significant psychological repercussions and necessitates significant financial and technological investment [5]. The treatments options for skin cancer are determined on the basis of disease progression, which includes conventional therapies such as surgical excision [6] and chemotherapy and newer therapies such as radiation, photodynamic therapy (PDT), immunotherapy, or targeted therapy [7].

Nanocarriers are promising drug delivery system, with an excellent ability of rendering therapeutics drugs into the cancer site precisely and securely enhancing therapeutic outcomes and limiting systemic adverse drug reactions. Initially, skin cancer is restricted to the skin's epidermal layer thus, topical application of drugs in the affected area is beneficial for the successful management of the skin carcinoma [8-9].

The novel nanoscale drug carriers explored for topical medication delivery in skin carcinoma include Nanoemulsions (NEs), vesicular carriers, polymeric micelles, solid lipid nanocarriers, metallic gold nanocarriers, dendritic polymers, carbon nanomaterials, and polymers based nanocarriers [10]. Among these, nanoemulsifying drug delivery systems have the potential to improve physico-chemical and pharmacological properties of chemotherapeutics agents. Despite having potential, their application is limited by their low viscosity, retention, and spreadibility, as well as lesser-known skin metabolomics and physical stability [11]. To resolve these problems and improve adhesion, suitable a gelling agent can be can be included to form nanoemulgel, which makes it suitable for transcutaneous application [12].

Nowadays, the attention has been increasing toward dietary phytochemicals obtained from whole fruits and vegetables, these compounds possess antioxidant, anti-inflammatory and anti-mutagenic properties against skin cancer [13]. SES (3,4 methylenedioxyphenol) is a safe, non-toxic natural phenolic compound obtained from roasted sesame seeds (*Sesamum indicum*) and sesame oil [14]. SES exhibits several pharmacological effects which includes radical scavenging property, mutagenic suppression, hepatoprotective effect, anti-inflammatory, geroprotective [15-17], anticarcinogenic properties in malignant melanoma skin cancer [18-21]. SES acts against skin cancer primarily through its pro-apoptotic mechanisms, antioxidant, anti-inflammatory, and as shown in animal models like DMBA-induced tumors [17]. The anticancer activity of SES can be elucidated through distinct pathways, such as decreasing Reactive oxygen species generation, suppressing membrane lipid peroxidation and macromolecular oxidative damage, elevating enzymatic antioxidants, inducing cancer cells

apoptotic pathway by disturbing mitochondrial integrity and inhibiting autophagic flux, and targeting various signal cascades that include the Tumor suppression cascade (p53),Mitogen-activated protein kinase module (MAPK), Stress-activated protein kinase route (SAPK), Protein kinase B signaling conduit path (PI3K/AKT), Tumor necrosis factor signaling path (TNFα), Nuclear factor-kappa B activation route (NF-κB), Peroxisome proliferator-activated receptor(PPARγ), Apototic protease activation (caspase-3), Antioxidanr response element pathway (Nrf2), endothelial nitric oxide synthase pathway (eNOS) and lipoxygenase enzymatic pathway (LOX) [22-25].

Although SES shown to exhibit considerable effects on different melanoma cell lines and have promising physicochemical characteristics such as high water solubility of about 38.80 mg/mL, a log P of 1.29 to 1.37 indicating balanced lipophilicity, and a pKa of 9.79, developing SES as anticancer agents is restricted because of various therapeutic constraints [26]. These challenges include poor oral bioavailability (around 35.5% ± 8.5), small t1/2 and fast systemic clearance, in addition SES shows rapid skin permeation to reach systemic circulation which further restricts its efficacy after administered topically [27-29]. Therefore, encapsulating SES within nanoemulgels can enhance the skin residence time thereby improving its chemopreventive efficacy against melanoma cells while avoiding first-pass metabolism [30]. Nanoemulgels are combination the advantages of NEs with nanoscale droplet sizes for enhanced skin permeation and bioadhesive properties of gels, significantly extending SES's residence time in dermal layers [12,31].

The current investigation explores underlying probable anti-skin cancer potential of the SES drug was further through the molecular docking studies. BRAF kinase crystal structure (PDB ID: 3OG7) was chosen as a subject of the current molecular docking experiment because of the importance of BRAF in the development and progression of the disease [32]. Further study focussed on developing, optimizing, and evaluating a nanoemulgel encapsulating SES for topical application, with an objective of improved pharmaceutical stability, dermal penetration, and controlled release for site specific cancer treatment, with enhanced therapeutic potential and fewer side-effects.

2. MATERIAL AND METHODS

2.1 Materials

SES was purchased from Sigma Aldrich (Steinhim, Germany), whereas Kolliphore oil (>99%), Tween 80 and polyethylene glycol 400 were purchased from G.L.R. Scientific Co., New Delhi.

Carbopol 940 (98%) was purchased, from Loba-Chemie (Mumbai, India). All the additional reagents, solvents and chemical employed such as triethylamine, methanol, etc., were of analytical grade. The in-silico studies were conducted by downloading the BRAF kinase crystal structure was downloaded from the protein databank (www.rcsb.org). The protein structure was prepared by removing the water of crystallization and co crystallized and checked for any missing atoms or residues by using the UCSF Chimera [33]. Ligand preparation and its energy minimization was done by employing the open-source software chemsketch 2025.2.5 [34]. Molecular docking and result visualization was performed using the open source software PharmoDock [35].

The pharmacokinetics and toxicity profile of SES was studied by PharmoADMET5. The chemical structure of SES was uploaded to the software in SMILES format. Various absorption, distribution, metabolism, excretion, and toxicity (ADMET) properties were predicted through integrated in silico models.

2.2 Methodology

2.2.1 Molecular Docking Studies

Underlying probable anti-skin cancer potential of the SES drug was further explored through the molecular docking studies. The BRAF kinase crystal structure (PDB ID: 3OG7) was downloaded from the protein databank (www.rcsb.org). The protein structure was then prepared by removing the water of crystallization and co crystallized and checked for any missing atoms or residues by using the UCSF Chimera [33]. Ligand preparation and its energy minimization was done by employing the open source software chemsketch3 2025.2.5 [34]. Molecular docking and result visualization was performed using the open source software PharmoDock [35].

2.2.2 In-Silico ADMET Profiling of the SES

The pharmacokinetics and toxicity profile of SES was studied by PharmoADMET [36]. The chemical structure of SES was uploaded to the software in SMILES format. Various absorption, distribution, metabolism, excretion, and toxicity (ADMET) properties were predicted through integrated in silico models.

The analysis includes the study of physicochemical properties, gastrointestinal absorption, skin permeation, blood-brain barrier penetration, water solubility, and druglikeness features [37]. Metabolic properties related to cytochrome P450 enzyme interaction were also analyzed.

Toxicological endpoints such as hepatotoxicity, mutagenicity, carcinogenicity, cardiotoxicity, and oral acute toxicity were predicted to assess the safety profile of SES

2.2 .3 Solubility Studies

SES solubility was measured in NE component including oil (Kolliphore-oil, Castor-oil, Olive-oil, Corn-oil, Coconut-oil, Soya-oil, Oleic-acid, Almond-oil, Eucalyptus- oil, Labrafac) as well as Surfactant and cosurfactant (Tween 80, Span 80, Span 20, Tween 20, Transcutol, Butanol, PEG 400, Propylene glycol, Glycerol and Ethanol). An excess amount of SES, was introduced to each vial sealed with 2 ml of respective oils and surfactants. Sealed mixture was then vortex-mixed for 10 min at maximum speed at room temperature to ensure proper dispersion of SES with the oils and surfactants until equilibrium (24 h). Vial was inspected for the undissolved drug residue, after 24 h and again SES in excess was added into the clear vial and again shaken for an another 24 h. Then mixtures underwent centrifugation at 3000 rpm for 10 min, supernatants were decanted into glass-vials, appropriately diluted with methanol, and analyzed using UV-visible spectroscopy at λ max 289 nm [38].

2.2.4 Method and Selection of Ratio for Optimization

Based on solubility studies NE preconcentrated were formulated comprising Kolliphor-oil as the oily phase, Tween-80 as a surfactant and PEG-400 as a cosurfactant. Surfactant and cosurfactant were pre-mixed as Smix at volume ratios of 1:1, 1:2, 2:1, 3:1, 4:1, and 5:1, then combined with oil in proportions from 1:9 to 9:1. Pseudo ternary phase diagrams were constructed via aqueous-titration method, where each oil-Smix mixture was slowly titrated with water under stirring to delineate NE formation regions and evaluate S/Cos effects on emulsion efficiency [39].

2.2.5 Experimental Design

For the optimization of the NE STAT EASE® Design of expert version 12.0.1.0 software was used. Under this response surface methodology was chosen and Central Composite Design was selected for the optimization of the NE [39]. The concentration of Kolliphore oil and conc of Smix were treated as independent factors, while globule size, Polydispersibility index (PDI) and entrapment efficiency were as dependent response. Formulation were characterized with these responses with optimal parameters were selected on the basis of experimental results.

2.2.6 Preparation of SES loaded NEs

NE preconcentrates comprising Kolliphore-oil, Tween-80 as surfactant, and PEG 400 as cosurfactant was developed by aqueous-titration method. SES (15 mg) initially was dissolved in Kolliphore oil (6.5 mL) followed by the incorporation of Smix (2:1, 3.0 ml). The mixture was stirred gently to homogeneity followed by dropwise titration with aqueous phase under constinous magnetic stirring to form NE. The formulations were stored at ambient temperature until futher characterization [40].

2.2.7 Characterization of SES loaded NEs

2.2.7.1 Determination of Globule Size, Zeta Potential and Polydispersity Index (PDI)

The Anton Paar LitesizerTM 500, particle size analyzer was employed to measure the average globule size, zeta-potential, and polydispersity index (PDI) of the prepared SES-NE using dynamic light scattering (DLS). Appropriate volumes of the samples were diluted with deionized water to confirm the light scattering intensity remain within the instrument detection range. Analysis was conducted at controlled room temperature at 25°C, with each performed in triplicate. The PDI was obtained using the same instrument to assess the globule diameter of the NEs, while zeta potential reflected their electrophoretic mobility [41].

2.2.7.2 Entrapment Efficiency (EE)

The entrapment efficiency of the prepared SES-NE was determined by using UV spectrophotometric method. Formulations underwent ultracentrifugation at speed 12000 rpm for 60 mins, supernatants were decanted, diluted with phosphate buffer saline (PBS) and recentrifuged for 3 cycles to isolated unentrapped SES. The concentration of free drug SES in supernatants were analyzed by UV–Vis spectrophotometer (Shimadzu UV-vis 1700) at 289 nm and % entrapment efficiency (EE) was calculated as [42]:

$$\textbf{\% Entrapment efficiency} = \frac{\textbf{Total Sesamol added} - \textbf{free Sesamol}}{\textbf{Total Sesamol added}} \textbf{ x 100}$$

2.2.7.3 Scanning Electron Microscopy, (SEM)

Surface topography of SES-NE was studied using a JEOL JSM-IT800, field emission scanning electron microscope. A drop of the NE was placed on aluminum stubs, air-dried overnight, and sputter-coated with gold-palladium prior to imaging [43].

2.2.7.4 In Vitro Drug Release

In vitro release testing of SES-NE employed the dialysis bag technique within a Franz diffusion cell assembly. One milliliter of the selected formulation was enclosed in a pre-soaked dialysis membrane (MWCO 12-14 kDa), which was then suspended in 25-50 mL receptor compartment containing phosphate-buffered saline (pH 5.5, 37±0.5°C) under continuous magnetic agitation at 100 rpm. Samples (1 mL) were withdrawn at fixed intervals of 0.5, 1, 2, 4, 8, 12, and 24 hours and immediately replenished with equivalent fresh buffer volumes, and quantified for released SES via UV spectrophotometry at λ_{max} 289 nm using a pre-established calibration standard [44].

Cumulative percent drug release was determined by the formula:

% Cumulative Drug Release =(released drug amount / initial drug content) × 100.

2.2.7.4 Differential Scanning Calorimetry

Differential scanning calorimetry, (DSC) Perkin Elmer Thermal analysis, Jade DSC V1, software version 9.0.1.0174)) was performed to assess the thermal behavior and drug-excipient interactions in optimized SES-NE. For the analysis, the samples were placed in a small sealed crucible and inserted into a temperature-controlled DSC cell. An empty crucible was placed in a separate cell as a reference. Both sample and reference was subjected to heating and cooling at a predetermined controlled rate. The differential the heat flow between the sample and reference was continuously monitored throughout the experimentation.The resultant thermographs were analysed to identify phase transitions, thermal behavior and reactions [45-46].

2.2.8 Preparation of SES -NEG

Optimized SES-NE was added into a 1% w/w Carbopol 940P gel base by gentle mixing. For the development of gel concentration of 1% Carbopol 940P (gelling agent) gel carrier. The gel base was developed by gradually incorporating Carbopol 940P into distilled with water continuous stirring using mechanical agitator at 1500 rpm for 30 min. The gel base was allowed to stand for 24 h in the dark to ensure swelling of the formulated base. This was followed by addition of optimal amount of Triethanolamine to maintain pH SES-NEG [47].

2.2.9. Characterization of SES-NEG

2.2.9.1 Measurement of pH

The pH of the formulated SES-NEG was estimated using calibrated digital pH meter equipped with a glass electrode at 25 ± 1 ◦C. For estimation, 1 g of formulation was dispersed in 10 ml of distilled water and thoroughly mixed and pH meter was allowed to equilibrate for 1 min before recording the measurement to ensure stable reading, this procedure was conducted in triplicate [48].

2.2.9.2 Spreadability

Gel spreadibility was evaluated using a customized wooden apparatus consisting of two parallel glass slides. One gram of gel sample was placed between the slides, with the upper slide hooked to a balance and loaded with 100 g weight, while the lower slide remained fixed.

The slides were separated over a fixed distance (L), and the time (t) it taken for complete separation was noted in triplicate. Spreadibility was determined by using following equation, where S, Spreadibility (g/sec), W is weight that applied, L is Length in cm and t is time taken for separation (sec) [49].

$$S = \frac{W\ XL}{t}$$

2.2.9.3 Rheological Analysis

Viscosity of gel formulation was determined using the Brookfield viscometer (spindle #64, 100 RPM,25 °C), having fixed outer cup mounted with sample, containing an immersed spindle that rotates. The size of the spindle used is selected based on viscosity of the sample- low viscosity larger spindles, and high viscosity smaller spindles. A stable dial reading was recored while spindle was rotating within the gel for an adequate amount of time, were recorded in triplicate [50].

2.2.10 Stability Study

To assess stability of SES-NEG, formulation was stored at different storage conditions including room temperature (25±2°C/60±5% RH), accelerated (40±2°C/75±5% RH), and refrigerated (4±2°C) environments for six months as per ICH guidelines. To evaluate formulation stability parameter such as physical appearance, viscosity, and pH were observed at 0, 1, 2, 3, and 6 months [51]

2.2.11 *Ex vivo* permeation study

Ex-vivo drug permeation study was performed using a modified Franz diffusion cell using rat abdominal skin. The prepared skin was then fixed onto a Franz diffusion cell, stratum corneum facing up toward the donor side and the dermis facing the receptor compartment below. The receptor chamber was filled with buffer and kept at 37±0.5°C, with constant stirring to keep conditions uniform. One gram of the SES-NEG was applied evenly across the skin surface in the donor compartment. Samples (1 ml) were drawn from the receptor fluid at set time points, with fresh buffer added back each time to preserve sink conditions throughout the experiment. These samples were filtered, diluted as needed, and quantified by UV spectrophotometry at 289 nm [41].

2.2.12 % Cell Cytotoxicity

Cell cytotoxicity of A375 human melanoma cultured in 96-well plates was determined by employing MTT assay to assess the effect of SES-NEG. Formulations at concentrations from 10 to 1000 µg/mL were applied to cells for 24-48 hours, then treated with MTT solution. After dissolving the purple formazan crystals in DMSO, absorbance was read at 570 nm. Viability percentage was calculated against untreated cell controls, and cytotoxicity obtained by subtracting viability from 100 [41, 52].

2.2.13 In Vivo Studies

Animal were received after approval from the Institutional Animal Ethical Committee at Despande Laboratories, Bhopal (Protocol No. CPCSEA No.-1582/PO/RE/S/11/CPCSEA).

2.2.13.1 Acute Dermal Toxicity

Acute dermal toxicity of SES-NEG was evaluated per OECD Guideline 402. A limit dose of 2000 mg/kg body weight was uniformly applied over ~10% shaved dorsal skin area of Wistar rats (n=5/sex), covered with occlusive gauze patch and non-irritant tape for 24 hours. Residual formulation was removed with lukewarm water post-exposure. Animals were observed individually for dermal reactions (erythema/edema scored per Draize scale), behavioral changes, and systemic toxicity at patch removal, then daily for 14 days. Morever, histopathological changes were evaluated by preserving specimens and performing the histopathological studies on the major organs of both the control and the drug treated group-rats ie lungs, heart and kidneys [52].

2.2.13.2 Skin Irritation Study

The dorsal area of each rat was shaved carefully without damaging the skin 24 hours before application. For testing SES-NEG was applied to the intact skin of designated animals. Approximately 0.5 g of formulation was homogenously spread over a are of 2× 2 cm and gently covered with a gauze patch to prevent removal. Animals were observed at 1, 07, 14, days after application to detect any visible signs of skin irritation such as erythema, edema, or other visible dermal reactions, further, histopathological analysis to assess the changes in the skin morphology. The experimental study was conducted in accordance with ethical standards for proper care and handling of laboratory animals, and observations were carefully recorded meticulously to determine the epidermal compatibility of formulated SES-NEG [52-53].

RESULT & DISCUSSION

3. 1 Molecular Docking studies

Molecular docking was carried out to analyze the binding affinity and interaction profile between the SES and the BRAF kinase (PDB ID: 3OG7), which is an important target for drugs to inhibit the proliferation of melanoma. The docking procedure was validated by employing the known reference ligand from the crystal structure.

The reference ligand displayed a binding affinity of −11.2 kcal/mol and generated some stabilizing interactions inside the active site of BRAF kinase. Hydrogen bond interactions were formed with Gln82 (2.98 Å), Cys84 (3.01 Å), Gly145 (3.02 Å), and Asp143 (3.04 Å), while some contact interactions were formed with Thr81 (2.98 Å) and Leu57 (3.17 Å). These interactions greatly help in stabilizing the ligand inside the ATP binding pocket of BRAF kinase. Two-dimensional (2D) and three-dimensional (3D) molecular interaction as shown in **Fig. 1** of the co-crystallized reference ligand docked within the active site of BRAF kinase (PDB ID: 3OG7). D interaction diagram that shows the main hydrogen bonds, as well as hydrophobic and van der Waals interactions formed between the ligand and the amino acids.. Also, 3D structure shows the spatial orientation of the ligand within the binding pocket, indicating its favorable accommodation in the ATP-binding site. Key amino acid residues involved in stabilizing the protein–ligand complex are labeled to provide a clear understanding of the binding interactions. These interaction profiles were generated to validate the molecular docking protocol by confirming the reproducibility of the experimentally observed binding mode before performing virtual screening.

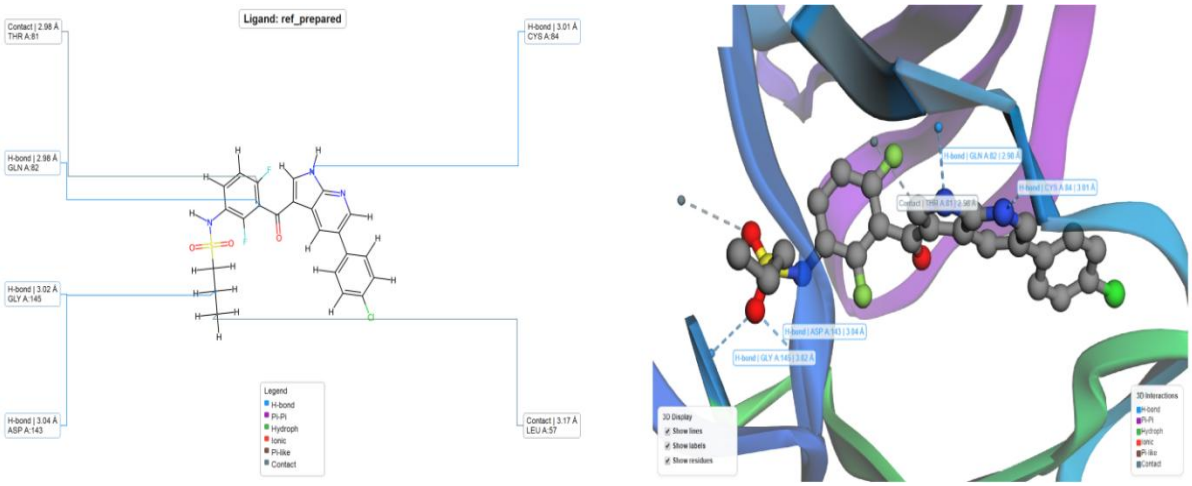


Figure 1: 2D and 3D molecular interaction diagrams of the co-crystallized reference ligand docked in the active site of BRAF kinase (PDB ID: 3OG7), showing key hydrogen-bond and contact interactions with the surrounding amino acid residues.

It should be noted that the binding affinity of SES was equal to −10.7 kcal/mol, which was rather similar to the binding affinity of the reference ligand. In addition, the docking procedure showed the establishment of hydrogen bond interaction between the molecule and Ala33 (2.87 Å), Ile79 (2.89 Å), Lys35 (3.21 Å), and Asp143 (3.08 Å). Hydrophobic interaction (Thr81, 3.53 Å) and contact interaction (Val34, 3.68 Å) contributed additional stability to the ligand inside the binding pocket. It should be also mentioned that Asp143 and Thr81 interacted both with SES and the reference ligand, indicating that SES binds to the same area of the binding pocket of BRAF kinase as the reference ligand does. **Fig. 2** represents the 2D and 3D interaction profile of the SES drug with target receptor.

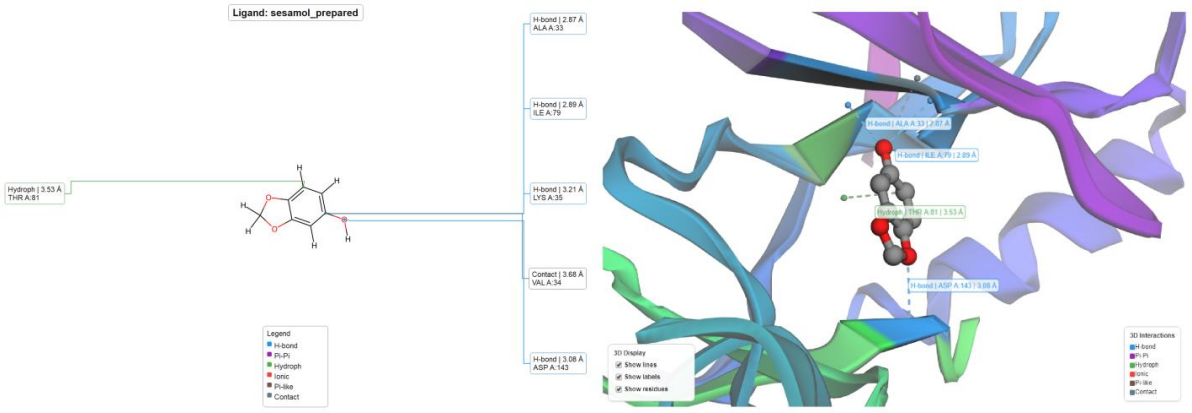


Figure 2: 2D and 3D molecular interaction diagrams of SES docked in the active site of BRAF kinase (PDB ID: 3OG7), showing key hydrogen-bond and contact interactions with the surrounding amino acid residues.

Although the docking score of SES differs from the docking score of the co-crystallized ligand by only 0.5 kcal/mol, the molecule of SES showed a good ability to create several hydrogen-bonds inside the catalytic pocket. It is worth noting that Asp143 interacts not only with the reference ligand but also with SES.

From the molecular docking studies, it is clear that the binding affinity of SES towards BRAF kinase is strong, and it can bind with the important residues involved in inhibiting the kinase enzyme. From the similar docking scores and conserved interactions seen with the reference compound, there is a good chance that SES can act as a good candidate in melanoma treatment. This study offers molecular evidence for the anti-cancer properties of SES and needs to be investigated further using molecular dynamics studies. The comparative result of the molecular docking of the co-crystalized ligand and the SES is given in the Table 01.

Table 01: Comparative molecular docking results of SES and the co-crystallized reference ligand against BRAF kinase (PDB ID: 3OG7)

Ligand	**Binding Affinity (kcal/mol)**	**Interacting Residue**	**Interaction Type**	**Distance (Å)**
Reference Ligand	**−11.2**	Gln82	Hydrogen Bond	2.98
		Cys84	Hydrogen Bond	3.01
		Gly145	Hydrogen Bond	3.02
		Asp143	Hydrogen Bond	3.04
		Thr81	Contact Interaction	2.98
		Leu57	Contact Interaction	3.17
SES	**−10.7**	Ala33	Hydrogen Bond	2.87
		Ile79	Hydrogen Bond	2.89
		Lys35	Hydrogen Bond	3.21
		Asp143	Hydrogen Bond	3.08
		Thr81	Hydrophobic Interaction	3.53
		Val34	Contact Interaction	3.68

3.2 In-silico ADMET profiling of the SES

Pharmacokinetics and toxicology studies on SES were conducted using PharmoADMET to check the drug-like nature and safety of SES as a skin cancer therapeutic candidate. Molecular descriptor study found that the molecule possessed a molecular weight of 138.12 Da, LogP of 1.12, and TPSA of 38.69 Å², which indicates good physicochemical properties. The compound contains one hydrogen bond donor and three hydrogen bond acceptors, which is within the limits acceptable for orally active drugs.

Druglikeness study confirmed that SES met all the criteria for Lipinski's rule of five and Veber's rules without having any violation, suggesting good oral bioavailability potential. Also, the compound has a QED value of 0.5834, indicating good drug likeness. Hence, the results obtained suggest good potential for developing this drug.

ADME studies predicted good gastrointestinal absorption along with high Caco-2 permeability, indicating good membrane transportability and absorption. Also, the compound exhibited good aqueous solubility (LogS = −2.0). It is unlikely that the compound will act as a P-glycoprotein substrate and also inhibit P-glycoprotein activity, hence making it less likely to develop resistance via a transporter-mediated mechanism. Also, there is less plasma protein binding in the compound.

The ADMET profiling showed low risk of interaction with the majority of cytochrome P450 isoforms like CYP3A4 and CYP2D6; thus, a lower risk of metabolic interactions with other drugs is expected. A moderate brain barrier permeability suggests possible penetration into the central nervous system.

Toxicity profiling revealed only one structural alert, which can be related to the phenolic group within SES. However, while phenols can sometimes exhibit oxidative reactions, the toxicity of the compound was estimated as low. SES received PharmoScore 90/100 with 100% prediction confidence, which speaks about the high quality of pharmacokinetic and safety properties of the compound.

Additionally, the ADMET results were confirmed by the PharmoGlyph radar, which showed favorable value for absorption, drug likeness, metabolism, and excretion, together with relatively low toxicity risk **(Fig. 3)**. Considering the above information, it can be concluded that the pharmacokinetic and safety properties of the compound are favorable enough for further studies and possible development into the drug against skin cancer. Overall summary of the I*n Silico* ADMET profiling of the SES is illustrated in the **Table 02**.

Table 02: Predicted ADMET characteristics of SES generated using PharmoADMET, including physicochemical parameters, drug-likeness, pharmacokinetic properties, toxicity prediction, and overall PharmoScore.

Property Category	Parameter	Result
Physicochemical	Molecular Weight (Da)	138.12
	LogP	1.12
	TPSA (Å²)	38.69
Drug-Likeness	Lipinski Rule	Passed
	Veber Rule	Passed
	QED Score	0.583
Absorption	GI Absorption	High
	Caco-2 Permeability	High
Distribution	BBB Permeability	Moderate
	Plasma Protein Binding	Low
Metabolism	CYP3A4 Risk	Low
	CYP2D6 Risk	Low
Excretion	Solubility	Good
Toxicity	Structural Alert	Phenol
Overall Assessment	PharmoScore	90/100

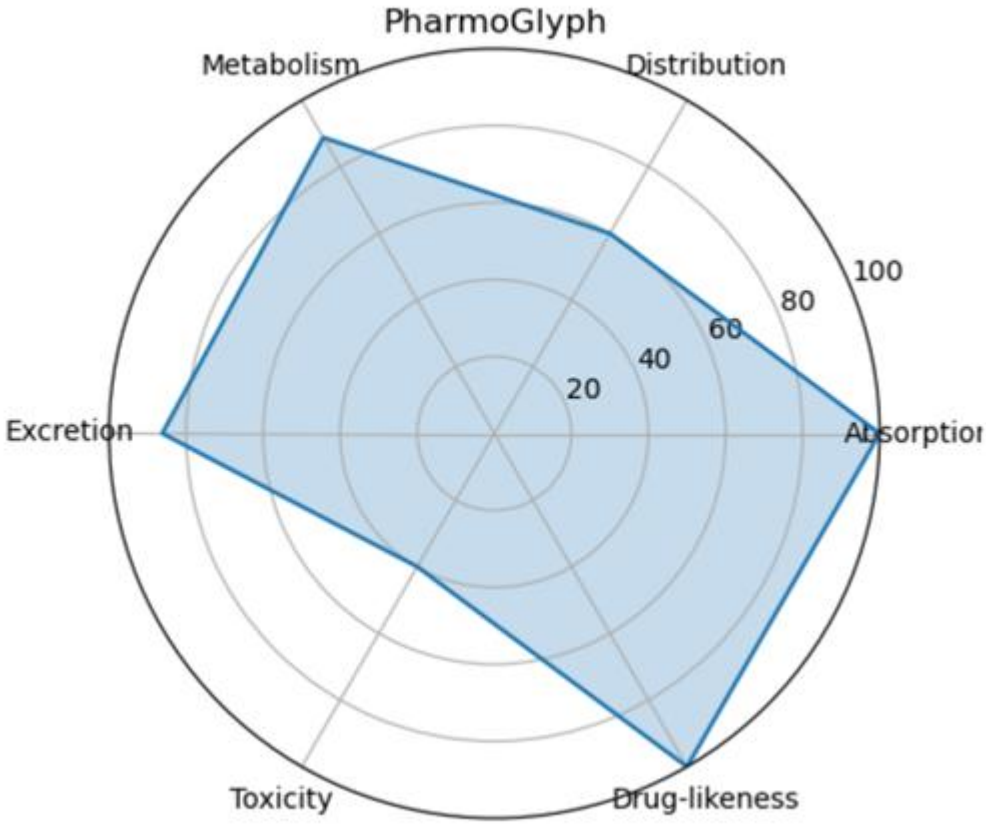


Figure 3: PharmoGlyph radar plot illustrating the predicted ADMET profile for SES generated using software PharmoADMET. The radar chart shows the relative scores for the six major pharmacokinetic domains, including absorption, distribution, metabolism, excretion, toxicity, and drug-likeness.

3.3 **Solubility Studies**

The solubilizing ability of SES was evaluated in various oils, surfactants, and cosurfactants with results are depicted graphically, in **Fig. 4**. Amongst tested oils, SES showed higher solubility in Kolliphore oil (6.91±0.049 mg/mL). Tween 80 and PEG 400 exhibited optimal solubilizing capacity and therefore utilized as surfactant and cosurfactant respectively for nanomulsions development.

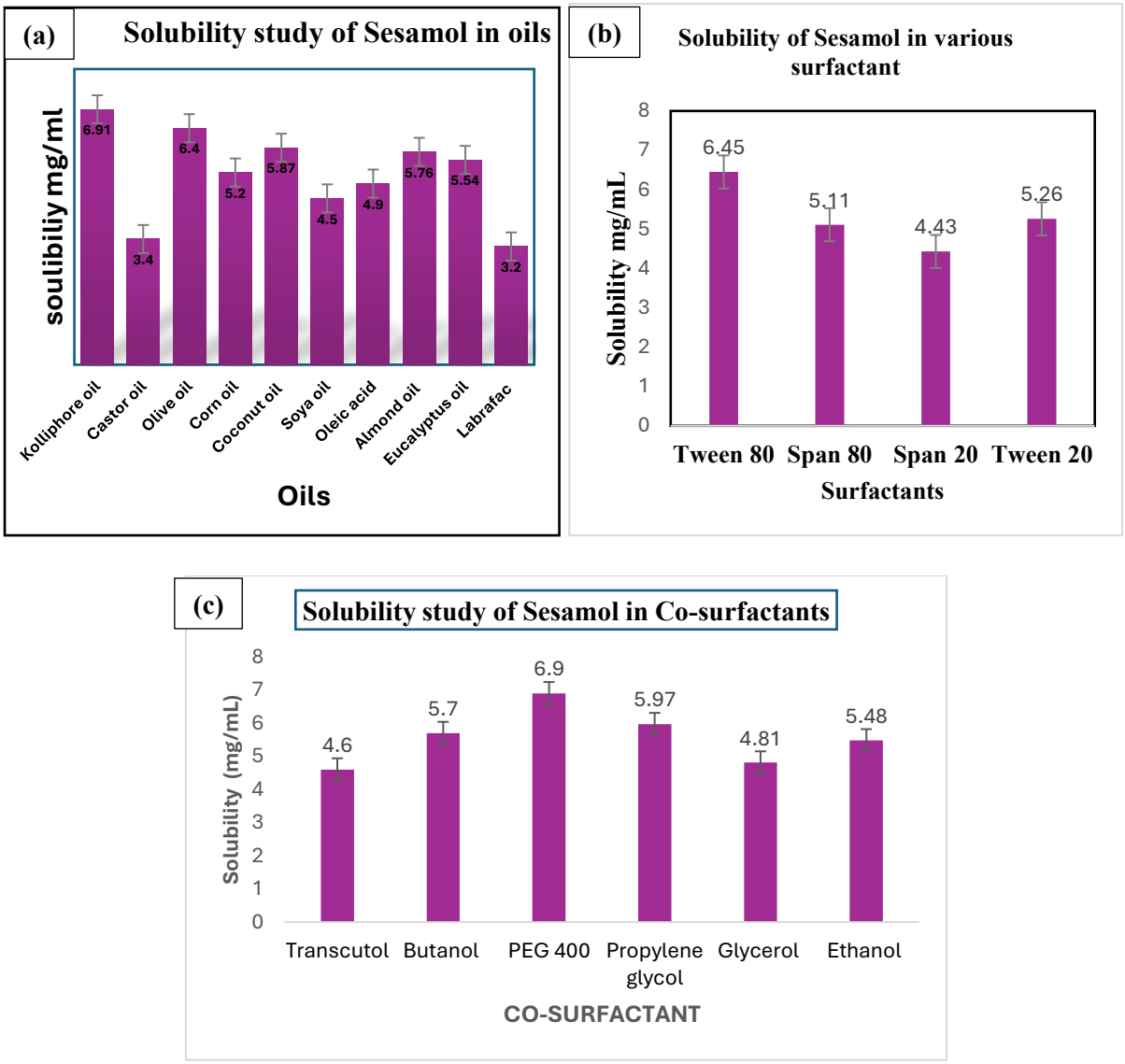


Figure 4: Solubility of SES in different (a) oils, (b) surfactants, and (c) cosurfactants, determined to identify suitable oil and Smix for nanoemulsion formulation. Data are presented as mean ± SD (*n* = 3).

3.4 Method and Selection of Ratio for Optimisation

The pseudo-ternary phase diagrams were constructed to identify the blend of excipients (ratio of oil phase and Smix) that give maximum NE region in the diagram and maximum dilutable lines. The phase diagrams for different Smix ratios are presented in **Fig. 5.**

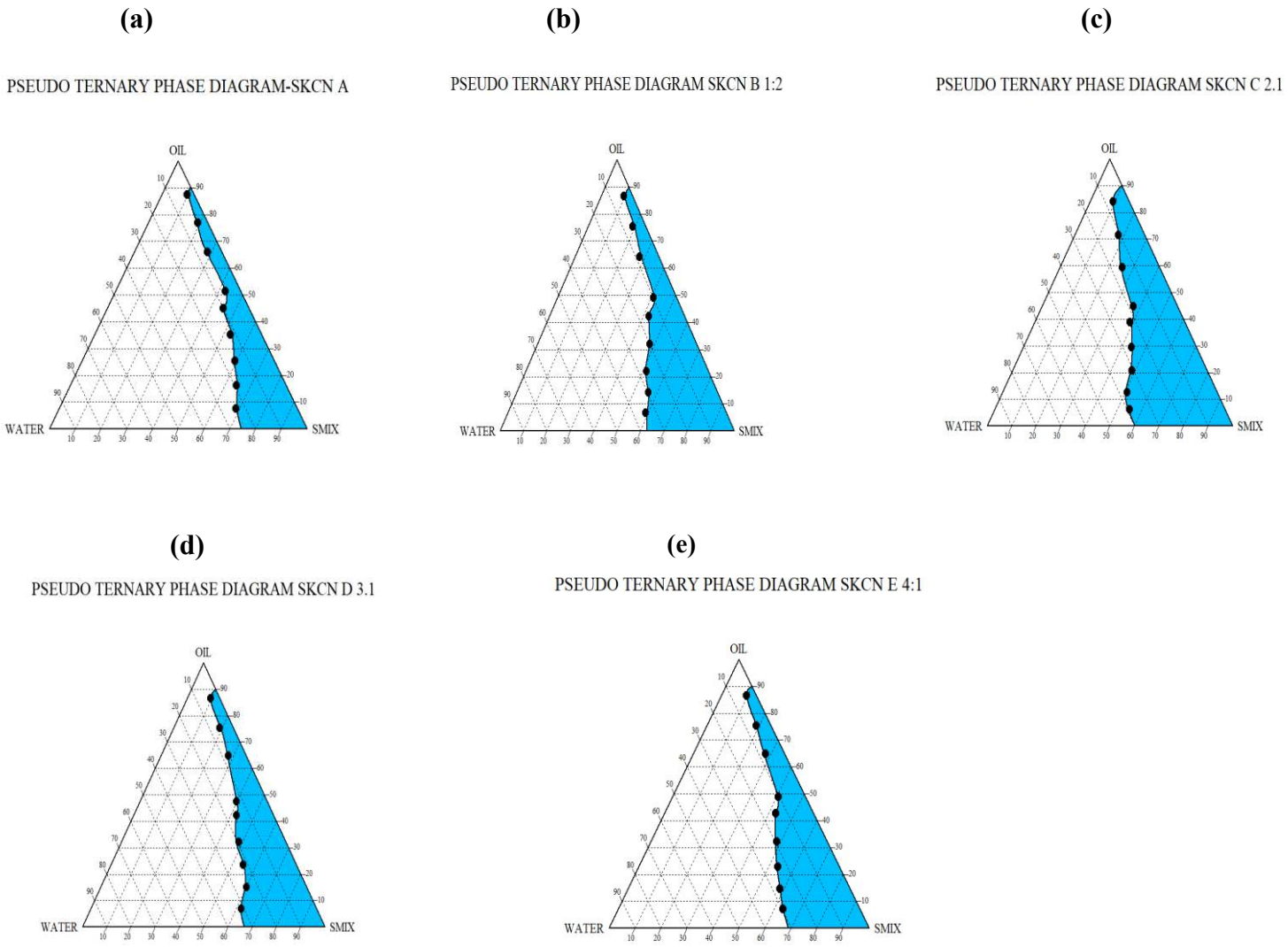


Figure 5: Pseudo-ternary phase diagrams showing NE regions (shaded) for oil, Smix, and aqueous phases at surfactant:cosurfactant ratios of (a) 1:1 (SCN-A), (b) 1:2 (SCN-B), (c) 2:1 (SCN-C), (d) 3:1 (SCN-D), and (e) 4:1 (SCN-E). The diagrams were constructed to study the effect of Smix composition on the extent of the NE region and to identify the optimum formulation composition for successive NE formulation.

The Nanoemulsion region (shaded area) was calculated and fully dilutable lines were identified in each phase diagram [54-55]. From the phase-diagram maximum NE region was found SCN-C: (Surfactant and Cosurfactant in 2:1) and and SCN-D (Surfactant and Cosurfactant in 3:1)) as compared to other Smix ratios. It shows that at higher surfactant amount in Smix, produces larger NE regions. In SCN-C, there is less surfactant amount (58%v/v surfactant) as compared to SCN-D (64 %v/v surfactant), hence we selected NE formulations, from SCN-C batch for further formulation development and characterization.

3.5 Optimization of SES loaded Nanoemulgel using Design of Expert (DoE)

An Design Expert Software, was used as an optimization tool to reduce formulation variability and achieve stable product with uniform, particle size and stability.

After pooling of data, statistical analysis was carried out and p-values, and model F-values for the response value; mean globule size (nm), PDI and entrapment efficiency (%EE) values, wss determined using Analysis of Variance (ANOVA). Y1 (mean globule size), Y2 (PDI) and Y3 (%EE) ranged between 206.9-230.4 nm, 0.10.6-0.223 and 54-90% respectively. Sequential model comparison, sum of squares analysis, lack of fit tests, and model statistics identified linear models as optimal for all responses. Linear models showed significant sequential p-values (<0.01) over quadratic/2FI, high R^2 values (0.89-0.95), excellent Adjusted/Predicted R^2 agreement (<0.2 difference), and adequate precision (>10) without aliasing or significant lack of fit. ANOVA confirmed model significance (particle size F=24.49 p=0.0013; PDI F=19.42 p=0.0024; EE F=56.62 p=0.0001), validating their suitability for SES NE optimization within the explored design space.

The signal-to-noise ratio was evaluated to assess the adequacy of the model precision, with values greater than 4 being considered acceptable. Adequate precision for responses Y1 (particle size), Y2 (PDI), and Y3 (entrapment efficiency) was found to be 12.114, 10.583, and 18.412, respectively. The predicted R^2 of Y1 (particle size), Y2 (PDI), and Y3 (entrapment efficiency) was found to be 0.7604, 0.7361, and 0.8896, respectively, indicating adequate signal. Three-dimensional plots (3D-Plot) obtained after Central Composite Design is depicted in **Fig. 6.**

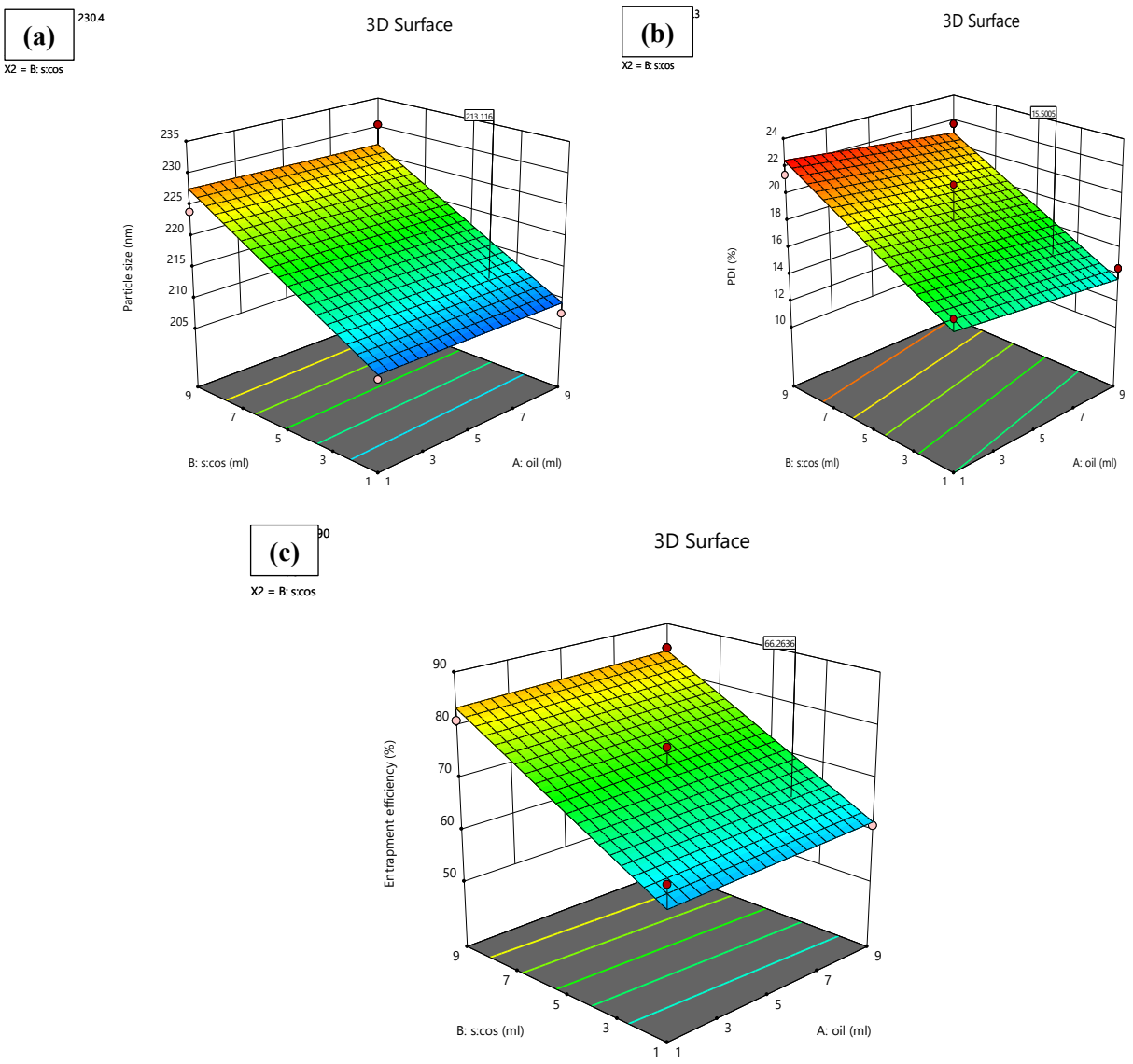


Figure 6: Three-dimensional response surface plots generated using the Central Composite Design (CCD) in Design-Expert® software, illustrating the influence of the independent formulation variables on (a) mean globule size, (b) polydispersity index (PDI), and (c) entrapment efficiency (%EE). The response surface plots were used to evaluate the effect of formulation variables and to identify the optimum formulation composition within the experimental design space.

3.6.1 Globule Size and PDI

The DLS technique was used to estimate globule size and PDI of optimized batch SES loaded NE, finding are displayed in **Fig. 7**. The finding suggests that the globule size and PDI were 215.0 ± 1.2 nm and 0.0273 ± 0.13, respectively. Subsequently, the particle-size must be smaller

than 250 nm for topical distribution, thus prepared NE was proposed appropriate for dermal application. In addition to improved skin penetration and minimizing systemic toxicity, formulation exhibits better kinetic stability than traditional emulsions [16, 56-57].

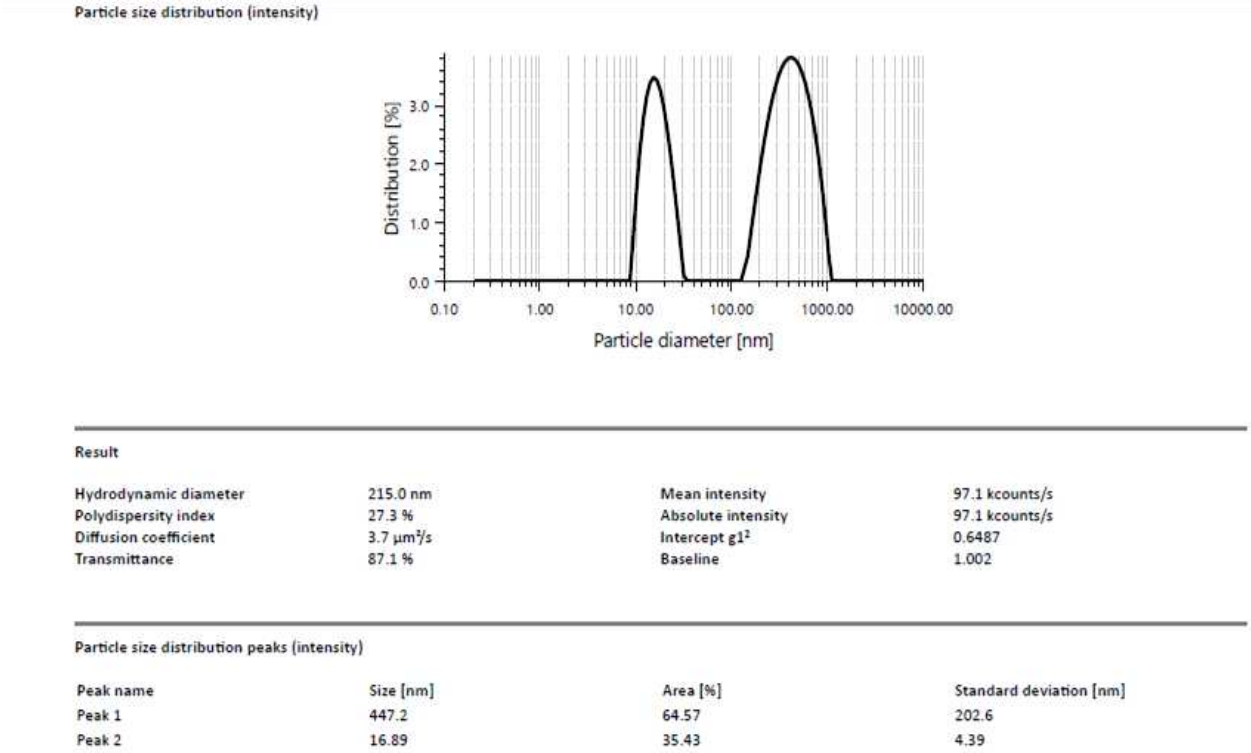


Figure 7: Particle size distribution and polydispersity index (PDI) of the optimized SES-NE determined by dynamic light scattering (DLS).

3.6.2 Zeta Potential

DLS technique was used to evaluate the zeta potential of the best optimized formulation **[Fig 8]**, the formulation exhibited negative zeta potential i.e -22 mv ± 0.89 mV. This might be due to the presence of anionic surfactants/co-surfactants which was absorbed at the oil-water interface with hydrophilic anionic heads oriented towards aqueous phase. The presence of surface negative zeta potential indicates that oil globules exhibit electrostatic repulsion that prevents droplet aggregation thereby stability the formulated NE [58-59].

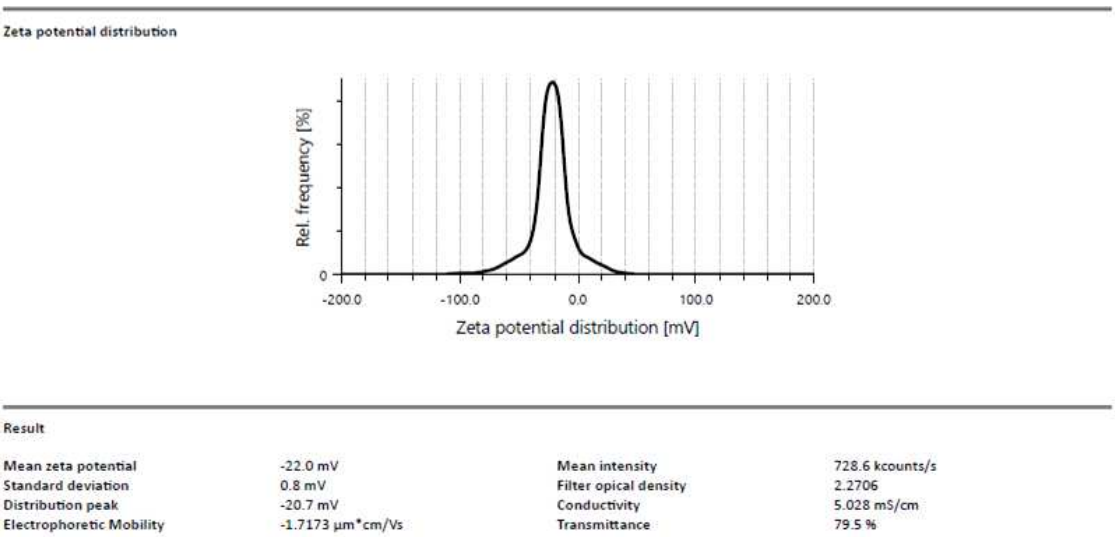


Figure 8: The zeta potential profile of the optimized sesamol-loaded nanoemulsion (SES-NE) assessed using DLS. This analysis was carried out to determine the surface charge and the colloidal stability of the optimized SES-NE.

3. 6.3 Entrapment Efficiency

The entrapment efficiency of the formulated SES-loaded NEs was calculated by using UV spectrophotometric method. The optimized SES-loaded NE demonstrates excellent entrapment efficiency (EE) of 81.8 ± 0.52%, indicating that 81.8% of the loaded SES is successfully encapsulated within oil droplets. The reason for the high %EE due to presence surfactant-co-surfactant mixture creating low interfacial tension that efficiently solubilizes SES within the oil phase ensuring sustained SES release for effective topical delivery [59-60].

3.6.4 Scanning Electron Microscopy

Surface morphology of optimized SES-NE was examined using a JEOL JSM-IT800, field emission scanning electron microscope. The SEM micrograph as shown in **Fig. 9** that revealed uniform distributed spherical nanosized particles with minimal aggregation, indicating good stability. Moreover, most of the particles were with a size less than 300 nm. Overall, the uniform nanoscale morphology confirmed the successful formation of the nanostructured system, which is favorable for enhanced surface area and improved drug release characteristics [61].

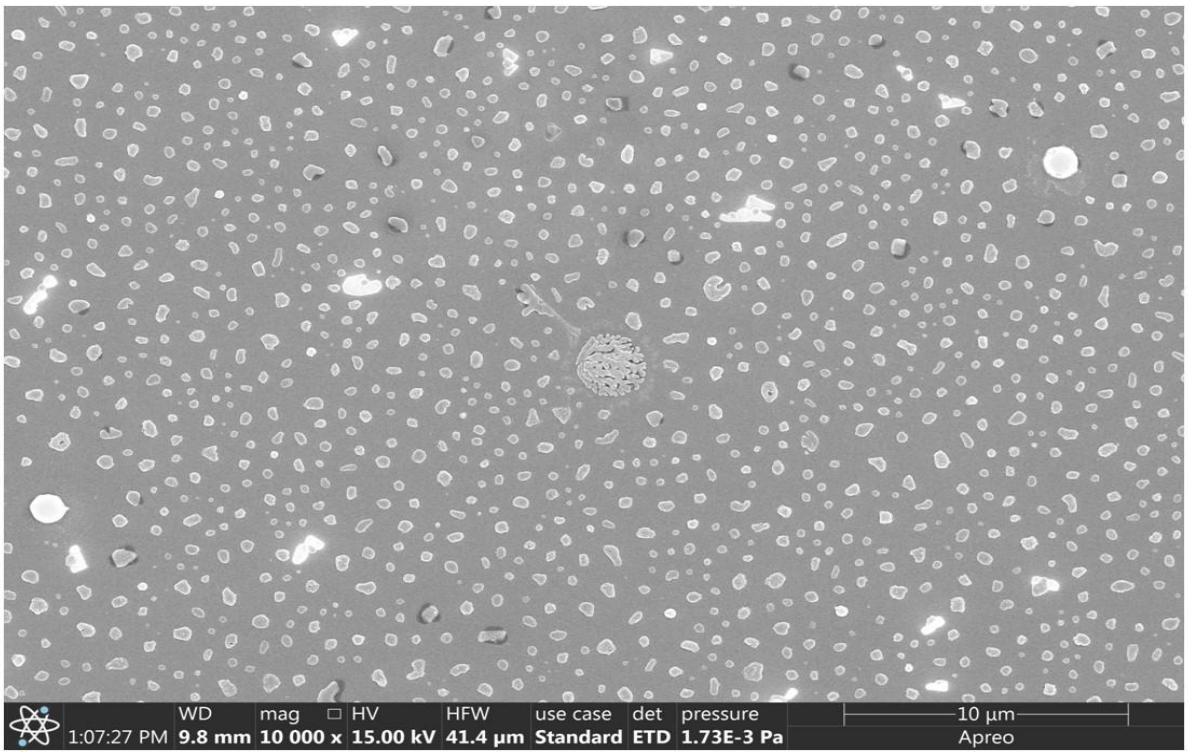


Figure 9: Scanning electron microscope (SEM) image of the optimized SES-NE, showing the morphology and distribution of the nanosized droplets within the formulation.

3.6.5 *In Vitro* Drug Release

Drug release kinetics of SES-loaded NEs was studied employing the dialysis bag technique within a Franz diffusion cell assembly. The in vitro drug release profile as shown in **Fig 10**, and SES loaded NE revealed sustained release behavior of the formulation and 85% from the formulation within 6 hours as compared with Pure SES which depicted only 12.26 %. An initial burst release in the early hours might be due to the presence of drug on the upper layer of the formulated nano-emulsion or it may be due to diffusion from outer layers. It has resulted by gradual and controlled release phase reaching approximately 95-98%. Overall, this sustained release characteristic is desirable for maintaining therapeutic drug levels over an extended period [62-63].

To investigate the drug release mechanism from optimized batch of SES loaded NE, the cumulative release data were fitted to four mathematical kinetic models (zero order, first order, Higuchi and Korsmeyer–Peppas) and the Hixson–Crowell cube root model.

Table 03: Regression equations and coefficient of determination (R^2) values obtained by fitting the *in vitro* drug release data of the optimized SES-NE to different kinetic models, including zero-order, first-order, Higuchi, Hixson–Crowell, and Korsmeyer–Peppas models.

Release Mechanism	Equation	R^2
Zero order	y = 7.943x + 16.758	0.824
First order	y = -0.1258x + 2.015	0.9616
Higuchi	y = 31.109x - 3.6238	0.9392
Hixson-Crowell	y = -0.2691x + 4.4844	0.9304
Korsmeyer-Peppas	y = -1.2759x + 2.0913	0.8825

The R^2 values for each model are summarized in **Table 03** and the corresponding plots are shown in **Fig. 11**. First order model was the best fit model for SES loaded NE drug release kinetics (R2 = 0.952). This implies that the release of drug from SES loaded NE was concentration dependent. Fickian diffusion had a significant contribution to the drug release from the SES loaded NE as depicted by the Higuchi model (R2 = 0.940).

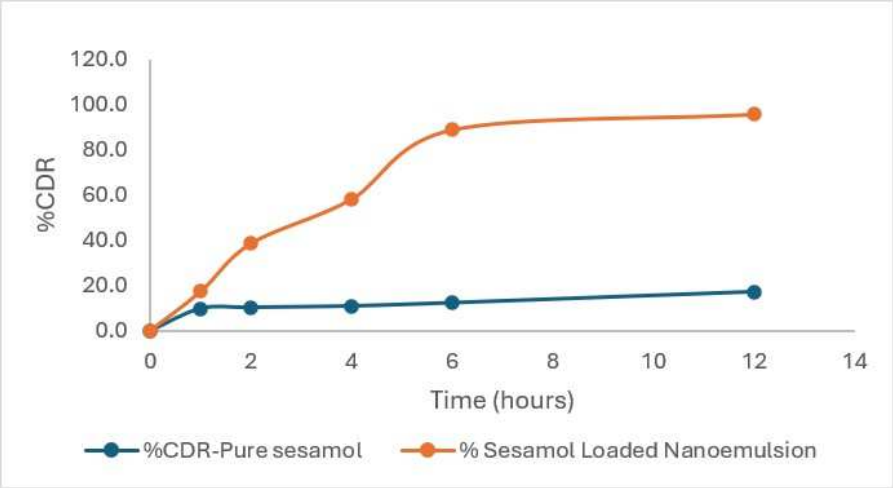


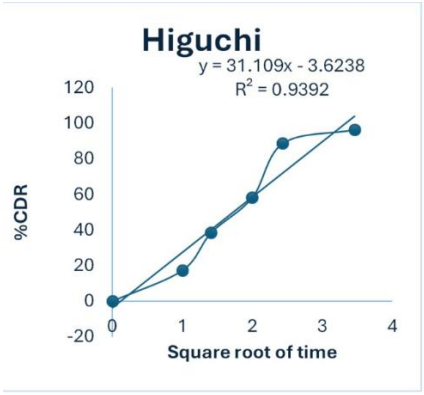
Figure 10: Cumulative Drug Release profile of Pure SES and Optimized Batch of SES-NE.



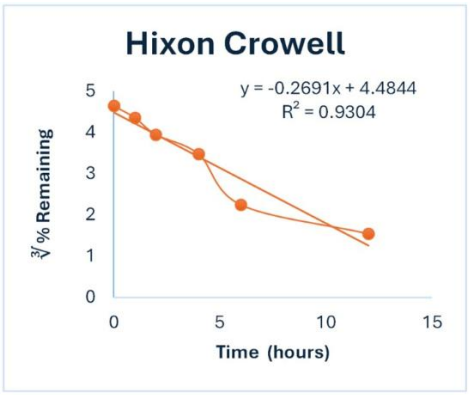
(a)



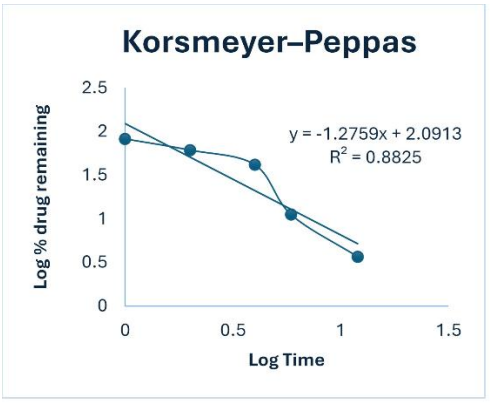
(b)



(c)



(d)



(e)

Figure 11: *In vitro* drug release mechanism of optimized SES loaded NE (a) Zero Order (b) First Order (c) Higuchi (d) Hixson-Crowell (e)Korsmeyer-Peppas. The plots were generated to evaluate the drug release kinetics and identify the predominant release mechanism of the optimized formulation.

3.6.8 Differential Scanning Calorimetry

The thermal analysis graph **[Fig 12]** depicts that pure SES melts sharply around 65–67.11°C, while the NE version shows altered melting due to encapsulation effects. Encapsulation in NE depresses and broadens the melting peak, lowers enthalpy, confirming SES is solubilized or complexed rather than crystalline. This enhances solubility, bioavailability and stability for pharmaceutical applications. Also, absence of pure SES peak in thermograph indicated suggests successful loading of SES in the NE [59].

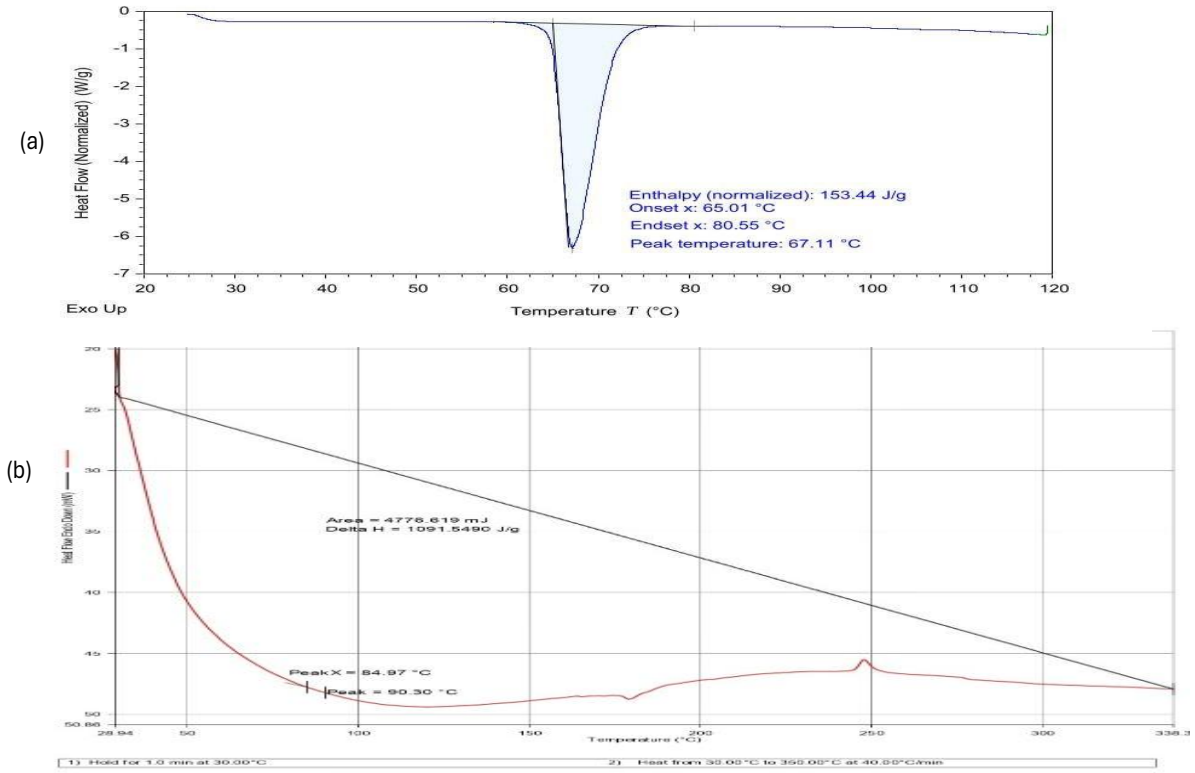


Figure 12: Differential scanning calorimetry (DSC) thermograms of (a) pure sesamol (SES) and (b) the optimized SES-NE. The thermograms were recorded to evaluate the thermal behavior of SES and to assess its physical state following encapsulation in the NE.

3.7 *In vitro* Characterization of SES loaded Nanoemulgel

3.7.1 Measurement of pH

The pH of SES-NEG formulation determined to 5.9 ± 0.024. As this approximates the human skin's pH of approximately 5, it indicates that the nanoemulgel will be non-irritating to the skin or cause any degradation from the SES [64].

3.7.2 Spreadability

The formulated nanoemulgel exhibited excellent spreading properties with an evaluated spreadibility value of 28.17 ± 0.015 g·cm/s², desirable for topical application. The high value also describes an optimal combination of viscous and elastic properties, meaning that they can be easily spreading over the surface of the skin while maintaining an even distribution of the drug [65].

3.7.3 Rheological Analysis

The viscosity of nanoemulgel containing SES was measured as 257.97 ± 12.32 cps which is an excellent viscosity value for topical semi-solid formulations; it enables a good spreading on skin, and the semi-solid formulation will hold its structure when applied to skin. This shows that Carbopol was successful in creating a gel-like system with shear-thinning characteristics allowing for the even distribution of SES to occur when the product is applied to the skin [50].

3.7.4 Stability Study

The stability study of formulated nanoemulgel conducted over six months under refrigerated (4–8°C/75% RH), room temperature (25±2°C, /60±5% RH), and accelerated (40±2°C, /75±5% RH), results are obtained are represented in Table 04. No significant changes were observed between the initial and final measurements (pH = 5.9±0.024; viscosity = 257.97–258.91 cP; spreadability = 27.98–28.17 g·cm/s) for all three stability conditions. The stable appearance, consistent composition, and overall lack of degradation demonstrate a low probability of phase separation and minor variations that are consistent with stability during long-term use [50].

Table 04: Stability data of SES-NEG

Stability parameter	**Month**	**pH**	**Viscosity**	**Spreadability**
4-8 °C with 75% RH	1	5.9±0.024	257.97±12.32	28.17±0.015
25 ± 2 °C with 60 ± 5% relative humidity	3	5.9±0.024	258.12±11.2	27.98±0.023
40 ± 2 °C with 75 ± 5% relative humidity	6	5.9±0.024	258.91±12.36	28.17±0.015

3.8 Ex-vivo Permeation

The ex vivo permeation study was performed using a modified Franz diffusion cell, and the cumulative amount of SES permeated from the optimized gel formulation was determined over 12 hours. The SES nanoemulgel demonstrated notably efficient skin permeation in the ex vivo study, with close to 92.5% of the dose passing through within 12 hours. Both the flux and permeability coefficient hit their highest points around the two-hour mark (189.75 µg/cm²/h and 0.1265 cm/h, respectively), after which they tapered off as the gradient driving drug movement across the skin gradually weakened, a pattern consistent with standard diffusion-based release kinetics rather than anything unusual. These finding (as depicted in **Fig. 13**) is suggested nanoemulgel have ability to facilitate permeation across stratum corneum layer of the skin as this drug delivery system have ability to disrupt the lipid bilayer organization of the stratum corneum and enhance drug diffusivity through the skin barrier due to incorporation of nanosized emulsion droplets and surfactant components.

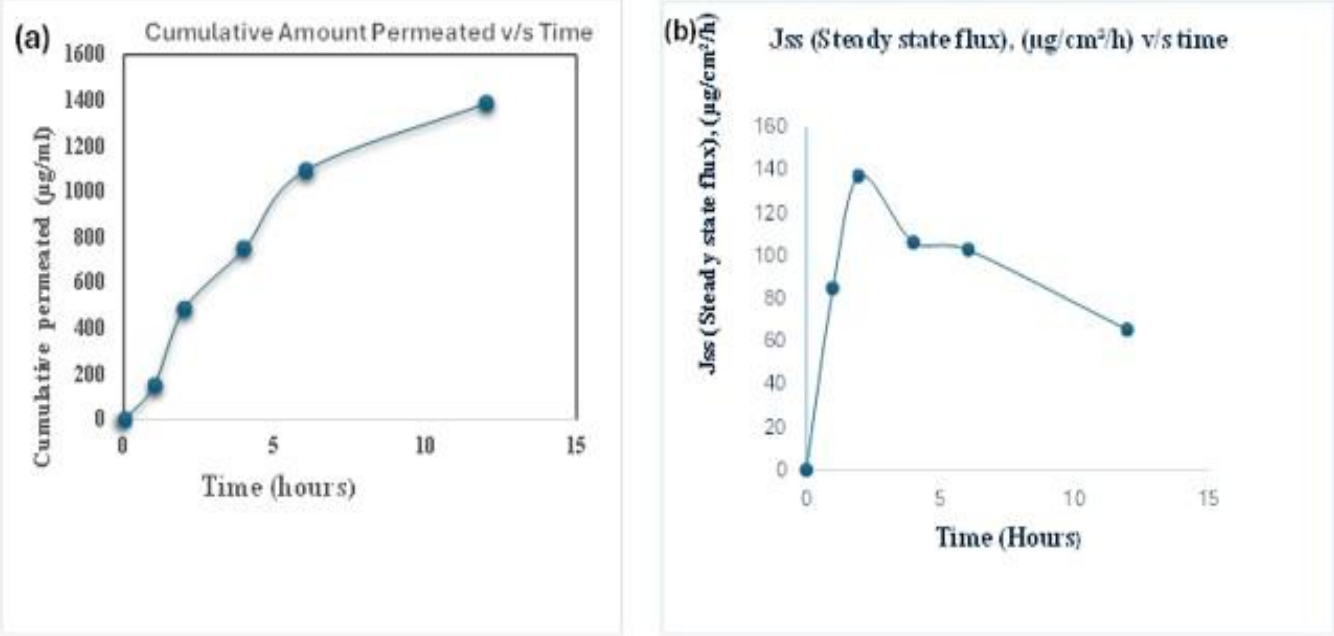


Figure 13: (a) Ex vivo cumulative permeation profile of SES from the optimized SES-NEG, (b) Steady state Flux profile of SES permeation from the SES-NEG.

3.9 Percent Cell Cytotoxicity

The effects of pure drug and SES loaded nanoemulgel were assessed through cytotoxicity studies against human melanoma cell lines-A375. Results showed (Figure 14) that SES-NEG significantly increased cytotoxicity compared to SES alone against human melanoma cell lines A375, which could be due to improved solubility of SES within the nanoemulsifying agent and

improved uptake of the drug into cells along with sustained release of drug from the gel matrix; all of these results lead to greater overall anticancer efficacy [66].

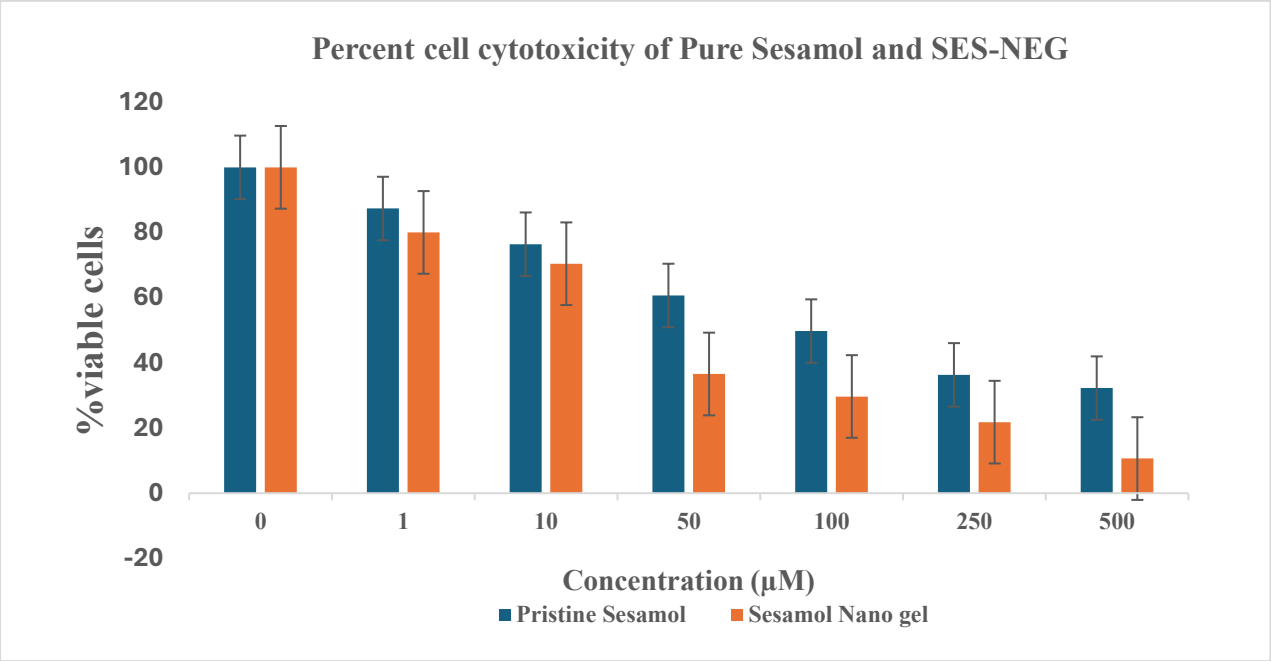


Figure 14: In vitro cytotoxicity of pure SES and SES-NEG against A375 human melanoma cells.

3.10 *In Vivo* Studies

Animal studies received approval from the Institutional Animal Ethical Committee at Despande Laboratories, Bhopal (Protocol No. CPCSEA No.-1582/PO/RE/S/11/CPCSEA).

3.10.1 Acute dermal toxicity studies for SES loaded naoemulgel

Acute dermal toxicity studies of SES-loaded nanoemulgel (NSMLG), with results summarized in **Table 5**, showed no mortality or significant clinical signs of toxicity over the 14-day period. All animals displayed normal behavior and consistent body weight gain throughout the observation [67]. The histopathological analysis (as depicted in **Fig. 15**) of the control and drug treated rats revealed that there were no significant changes in the morphological characteristics with the normal control and the drug treated groups. The main organs included for the analysis were heart, lungs and kidneys. The lung specimens showed normal alveolar structures with no thickening and no infiltered inflammatory cells are visible. The cardiac tissues were having properly aligned cardiac cells with normal morphological arrangements without any significant change when both the groups were analysed. The kidney tissues were analysed for any changes in glomerular shape and cellular structure which was found to be normal. Thus, it can be said

that the test drug formulation does not cause any significant morphological change when applied topically and can be a potential therapeutic measure for further investigation for the skin cancer.

Table 5: Body weight changes and Mortality

Group	Dose (mg/kg)	Rat No.	Sex	Day of Death	Body Weight (g)			No. dead/Tested
					0 Day	7 Day	14 Day	
A	2000 mg/kg	R1	F	--	185	192	200	0/3
	"	R2	F	--	190	198	205	
	"	R3	F	--	195	202	210	

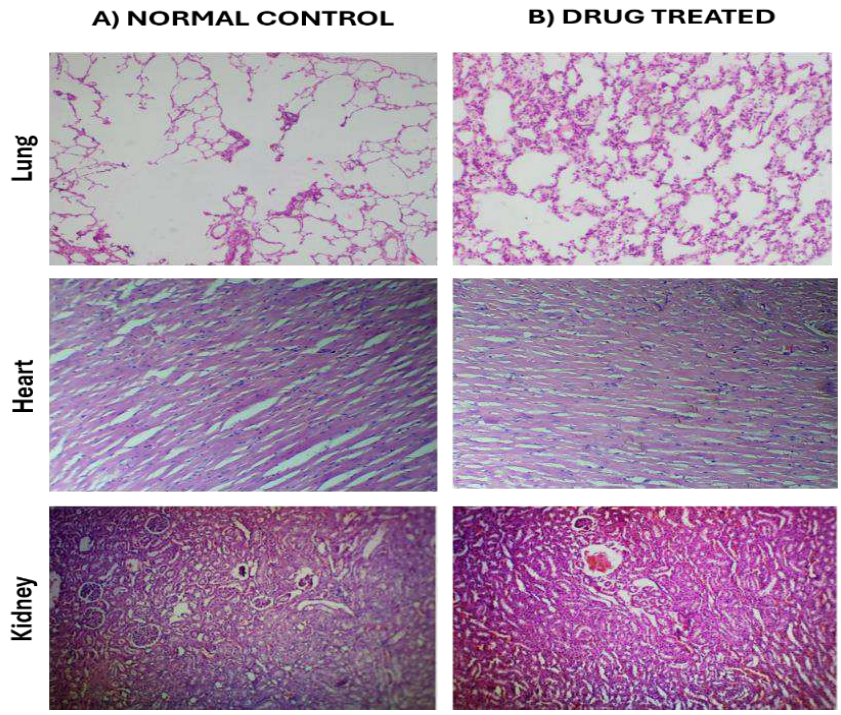


Figure 15. Histopathological analysis (A- Normal Control; B-Test drug) of tissues of different organs:Lungs, Heart and Kidney; showed there was no significant change observed within the two groups.

3.10.2 In vivo skin irritation Studies for SES loaded naoemulgel

The skin toxicity analysis was done using 14 day skin irritation test model on wistar rats. The drug treated group did not show any signs of irritation when the test drug was applied topically for a period of 14 days [68].

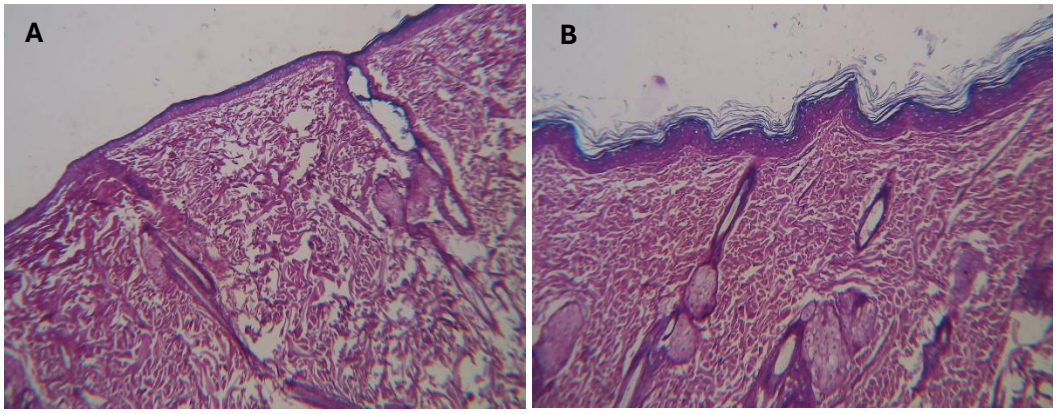


Figure 16: Histopathological analysis of skin tissues: (A) Normal Control group and (B) Drug treated group.

No swelling/edema or inflammation was visible on physical examination and the histopathological analysis also showed normal tissue morphology as compared to normal control, group rats. The epithelial layer was observed to have normal thickness with intact hair follicles and inside the upper layer, sebaceous glands were observed during the morphological evaluation of the skin tissues. These finding were comparable to the normal control group results and there was no significant change found in the morphological characteristics within the two different groups of the animals included in the study **[Fig. 16]**.

DISCUSSION

Melanoma is one of the most aggressive and resistant types of skin cancers owing to the complexity of molecular mechanisms behind it and problems associated with the effective transport of drugs through the skin barrier [69]. This situation demonstrates the necessity for development of advanced topical delivery systems that would increase local drug concentrations while decreasing their systemic exposure. The current investigation has demonstrated a successful combination of molecular modeling, in silico pharmacokinetics prediction, optimization of formulations, physicochemical and biological investigations to formulate a SES-NEG for topical treatment of skin cancer. Unlike previous research, which mainly emphasizes the development of formulations, in the current study, we have devised a translational pathway by relating the molecular interaction of SES with BRAF kinase enzyme, rational formulation design, increased dermal delivery, and better biological efficacy.

Molecular docking showed that SES has a high binding affinity towards BRAF kinase (−10.7 kcal/mol) which is quite comparable to that of the reference ligand used during crystallization. However, more importantly, the conservation of key interactions with Asp143 and Thr81 implies that SES interacts with the ATP-binding pocket of BRAF in a way that is highly similar to established BRAF inhibitors. This is due to the fact that the constitutive activation of BRAF kinase is one of the main molecular mechanisms of progression of melanoma through the MAPK pathway and the inhibition of this target is a validated approach for treatment [32]. These similar findings were obtained by Grauso et al. (2020), in silico study that focused on the interaction of vanicosides A and B from *Reynoutria sachalinensis* with BRAF V600E and MEK1 using molecular docking on A375 and SK-MEL-5 melanoma cell lines. Their study demonstrated favourable binding energies and critical residue interactions, which are comparable to the interaction profile observed for SES in the present investigation [70]. The docking results therefore provide a strong molecular rationale for the experimentally observed anticancer activity of SES against A375 melanoma cells. In addition, SES has been reported to regulate redox-sensitive signalling pathways, particularly the MAPK and Akt cascades, which function downstream of BRAF activation. This mechanistic evidence further supports its potential role as an antagonist of the BRAF signalling pathway [71]. When considered alongside its excellent PharmoScore and favourable ADMET characteristics, these findings collectively highlight SES as a pharmacologically promising candidate for the topical treatment of melanoma.

Notably, the effectiveness of topical therapy is not solely based on pharmacological efficiency but on effective delivery through the highly structured stratum corneum. As such, formulation optimization will be an important aspect in enhancing the performance of the topical therapy. Based on the results of solubility screening, the most appropriate formulation ingredients include Kolliphore oil, Tween 80, and PEG 400 since they have excellent drug solubilization ability. In addition, construction of pseudo-ternary phase diagrams revealed that the chosen Smix ratio created the biggest nanoemulsion region. This was an indication of good self-emulsification and thermodynamic stability. The use of Central Composite Design was useful in optimizing various formulation parameters with minimum variation in experiments. The reliability of this methodology is well supported by previous studies, Kumar et al. (2022) successfully employed a three-factor Central Composite Design (CCD) to optimize azilsartan

medoxomil-loaded nanoemulsions, demonstrating that response surface methodology can generate statistically robust and highly predictive models for pharmaceutical nanoformulations [72]. These findings are consistent with the present study, where the ANOVA results and predictive performance similarly confirmed the validity and robustness of the developed optimization model.

The optimized SES-NE showed a mean globule size of 215 ± 1.3 nm, a polydispersity index of 0.273 ± 0.013, a zeta potential of −22 ± 0.016 mV, and an entrapment efficiency of 81.8 ± 0.52%. These findings altogether signifies that the nanoformulation is physically stable, and has a narrow range of droplet sizes along with efficient encapsulation of the drug within. Being small-sized, the globules have a larger interfacial surface area which allows for greater interaction with the lipids present in the stratum corneum layer. This further helps in enabling the transport of drugs passively into the lower epidermal layers containing the melanoma cells. All the above-mentioned properties are in accordance with the physicochemical criteria of topical drug delivery. The obtained results are comparable to those reported by Geetha et al. (2015) for SES-loaded solid lipid nanoparticles (S-SLNs), which exhibited a particle size of 127.9 nm and a polydispersity index of 0.256. The relatively smaller particle size observed in their study can be attributed to the compact lipid matrix of solid lipid nanoparticles compared with the oil-in-water nanoemulsion system used in the present work [27]. Notably, the encapsulation efficiency exceeding 80% achieved in this study demonstrates the effectiveness of the selected oil–surfactant system in retaining sesamol within the formulation. These findings are in good agreement with the encapsulation efficiency of 88.21% reported for sesamol-loaded SLNs by Geetha et al. (2015) and Hashim et al. (2025) for sesamol-containing transliposomal gel 75.60 ± 3.68% [27,25].

The development of the optimized SES-NE was additionally confirmed by morphological and thermal analyses. Surface morphology of optimized SES-NE revealed uniform distributed spherical nanosized particles with minimal aggregation, indicating good stability. The thermal analysis using differential scanning calorimetry revealed that there was no presence of the clear melting endotherm of the crystalline drug due to encapsulation effects. Encapsulation in NE depresses and broadens the melting peak, lowers enthalpy, confirming SES is solubilized or complexed rather than crystalline. thus it is evident that the SES has been successfully incorporated into the lipid nanostructure.

The drug release studies confirmed the sustained release of the SES from the SES-NE formulation; the amount of the drug released was much higher compared to the pure drug. Kinetics analysis proved the predominance of first order release with Higuchi diffusion mechanism; therefore, the release of the drug depends mainly on diffusion controlled process in the matrix of the NE. This sustained-release profile is therapeutically advantageous for topical chemotherapy, as it may prolong drug availability in the epidermis and dermis, thereby reducing dosing frequency and potentially improving patient adherence. These release kinetics are consistent with those reported for the recently published 5-FU and SES- transliposomal gel, which showed sustained release of 82.52% and 86.28% for 5-FU and SES, respectively [25]. However, the self-emulsifying nanoemulsion system used in the present study offers additional practical advantages over liposomal formulations, particularly in terms of thermodynamic stability, ease of preparation, and scalability.

To improve suitability of optimized SES-NE for topical administration, it was incorporated into a Carbopol-based gel matrix to overcome several practical drawbacks inherent in the liquid nanoemulsion. The resulting SES-NEG formulation exhibited a skin friendly pH 5.9 ± 0.024, excellent viscosity, and spreadibility, which suggested that it can be applied effectively and ensure long-lasting contact with the skin. Notably, the addition of the optimized SES-NE to the gel base did not impact its stability and thus retained its delivery capabilities. The physicochemical properties of the SES-NEG formulation remained stable under different storage conditions, confirming its overall physical stability throughout the study period. The observed physicochemical characteristics are in good agreement with those reported for similar formulations in the literature. Jadhav et al. (2024) developed an imiquimod-loaded Carbopol-based nanoemulgel for topical skin cancer therapy that demonstrated comparable physicochemical properties, along with enhanced drug solubility, improved skin permeation, and increased therapeutic efficacy [60].

One of the most notable outcomes of the present study was the significant enhancement in the skin permeation of SES achieved with the SES-NEG formulation. The ex vivo permeation studies have shown that SES permeates through the skin efficiently, and the mechanism of its skin permeation can be considered as the combination of presence of the nanosized droplets with increased surface area and enhanced skin permeation properties provided by the surfactants and co-surfactant incorporated. This is attributed to the reason that nanoemulsion droplets interact with the intercellular lipid domains of the stratum corneum, resulting in

temporary destruction of the lipid domains organization and skin permeation of the drug. This mechanism has been extensively studied and reported in a numerous topical drug delivery system [25]. Comparable findings have been reported by Singh et al. (2026), who developed a wheatgrass extract-loaded nanoemulgel that achieved 95.08% skin permeation after 24 hours, along with enhanced dermal drug deposition. These results further highlight the ability of nanoemulgel systems to improve skin permeation [73]. In the current study, increased penetration of SES is highly important for maintaining adequate concentration of the drug at the site of action without excessive absorption into the body system is very important for the topical treatment of the condition.

It could be observed that the increased effectiveness of the SES-NEG system was demonstrated by its much higher cytotoxicity against A375 melanoma cells than that of free SES, indicating that nanoencapsulation improves the anticancer efficacy of this phytoconstituent. This can be concluded from the increasing number of studies that have revealed the potential for enhancing the efficacy of SES through nanocarrier-based delivery systems. Srisongkram et al. (2022) found that SES, sesamin, and sesamolin utilize different modes of cellular uptake and have different cytotoxicity profiles in SK-MEL-2 melanoma cells, which indicates that intracellular transport processes are an important determinant of their antitumor effect [21]. Nanoencapsulation could be used to address these issues and increase cellular uptake of SES. Similarly, Nair et al. (2022) demonstrated that SES-loaded nanosponges produced significantly greater in vitro cytotoxic and anti-inflammatory effects than free SES suspensions [19]. Consistent with these observations, Jahan et al. (2025) reported that a 5-FU and SES-loaded transliposomal gel achieved 90.38 ± 0.93% cytotoxicity against A431 cells at a concentration of 300 μM, compared with 77.60 ± 1.00% for the SES suspension [25]. The improvement observed in their study is comparable to the enhanced cytotoxic activity achieved with the SES-NEG formulation in the present investigation. The enhanced cytotoxicity observed with the SES-NEG formulation is likely the result of several complementary factors, including improved solubility of SES, increased cellular uptake mediated by the nanodroplets, sustained intracellular drug availability, and stronger molecular interaction with the BRAF kinase target .Earlier investigations have established that SES was able to induce activation of intrinsic and extrinsic apoptosis pathways, S-phase arrest in the cell cycle, and inhibition of colony formation in a dose-dependent way in lung adenocarcinoma, colon cancer, and hepatocellular carcinoma models. It is accompanied by the regulation of such signaling pathways as MAPK, Akt, JNK, and caspase-3 [74]. In view of the above, the increased availability of SES in the

A375 melanoma cells harboring the mutated BRAF protein would help boost these apoptosis-related pathway

The formulated SES-NEG exhibited an acceptable safety profile throughout the duration of the experiment. There were no indications of any systemic toxicity, skin irritation, or any histopathological changes after both acute and repeated topical application of the formula, implying that the inclusion of SES in the nanoemulgel did not affect its safety. In addition, the histological structure of the skin, heart, lungs, and kidney was maintained, suggesting good biocompatibility of the formulation. These findings are consistent with previous reports on lipid-based nanocarrier systems. Geetha et al. (2015) demonstrated that SES-loaded solid lipid nanoparticles provided enhanced skin retention with minimal transdermal permeation and showed no evidence of toxicity, which was attributed to the physiological lipid composition of the carrier [27]. Collectively, these findings suggested that the SES-NEG formulation offers an improved therapeutic profile by enhancing local drug delivery while maintaining systemic safety.

Altogether, the findings of the present study demonstrated that rational optimization of a SES-NEG can significantly improve its therapeutic performance while maintaining a favorable safety profile. The combined evidence from molecular docking supporting BRAF inhibition, favorable ADMET characteristics, systematic formulation optimization using pseudo-ternary phase diagrams and Central Composite Design (CCD), DSC-confirmed drug encapsulation, sustained diffusion-controlled drug release, enhanced skin permeation, increased cytotoxicity against A375 melanoma cells, and excellent dermal tolerability highlights the potential of the SES-NEG formulation as a promising candidate for topical melanoma therapy. Compared with previously reported sesamol-based nanocarrier systems, including solid lipid nanoparticles, nanosponges, and transliposomes, the present study provides a more comprehensive proof of concept by integrating a BRAF-targeted molecular rationale with a clinically relevant nanoemulgel delivery system for topical treatment of melanoma.

Despite promising results, there are several steps to be taken before considering clinical translation. Further validation in orthotopic melanoma models closer to physiological tumor microenvironment and in vivo demonstration of BRAF/MAPK pathway inhibition would be necessary. Moreover, comprehensive derma-kino- and pharmaco-kinetic analysis as well as evaluation of long-term efficacy under simulated conditions of chronic application will be important to perform. Another aspect for further investigation could be the influence of nano

formulation on the known melanogenesis inhibitory effect of SES in BRAF mutated melanoma cells. Considering all these points in future research will increase the translational potential of SES-NEG as a new promising and safe topical approach to melanoma therapy. This approach could also serve as an alternative or complimentary option for available systemic BRAF inhibitors, which have several restrictions including acquired drug resistance and toxicity associated with treatment.

CONCLUSION

Topical drug delivery to treat skin cancer is fundamentally constrained by the impermeable, densely keratinized nature of the stratum corneum, and the treatment options currently in clinical use are further limited by side effects such as scarring, systemic toxicity, and poor patient adherence. Formulations that combine adequate skin permeability with good cutaneous tolerability are therefore essential to address this gap. Plant-derived agents such as sesamol (SES) present an attractive option in this regard, as they tend to be non-toxic, non-irritating, and well tolerated by the skin while still exerting meaningful anticarcinogenic effects. This rationale was reinforced by molecular docking analysis, which showed sesamol binding tightly to the active site of BRAF kinase, with a binding energy of −10.7 kcal/mol anchored by interactions with the Asp143 and Thr81 residues. The resulting Pharmoscore of 90/100 reflected high confidence in this predicted binding mode, and the accompanying in silico ADMET evaluation further supported sesamol's suitability as a candidate for topical anticancer therapy.

Based on this molecular rationale, a sesamol-loaded nanoemulgel (SES-NEG) was successfully developed and optimized for topical delivery in skin cancer. The development and characterization of an optimized SES NEG for use as a topical application resulted in the following: a suitable physicochemical formulation containing a globule size range (173 to 215 nm); the average globule PDI was 0.273 to 0.353; the zeta potential was -22 mV; the entrapment efficiency 81.8%. The pH of the formulation was 5.9±0.024; the viscosity was 257.97±12.32 cP; the spreadability was 28.17±0.015 g.cm/s. The formulation was subjected to 6 months ICH stability testing (no degradation or phase separation). In vitro studies demonstrated sustained release (85% at 6 hrs), DSC confirmed molecular solubilisation,and significantly improved anticancer activity against A375 melanoma cell lines as compared to SES alone through

increased solubility, cellular uptake, and controlled delivery. *In vivo*, dermal safety studies demonstrated no irritation (PII score of 0.0) or systemic toxicity (LD50 >2000 mg/kg) establishing the use of SES loaded nanoemulgels as a stable, non-greasy, topical system for improved delivery of SES, an improved in skin retention and permeation, a reduced patient dependence on oral administration of SES, and offers an promising alternative to the current delivery systems used in treating skin carcinoma. Considering the improved physicochemical properties, favourable molecular docking profile, and robust *in-vitro/in-vivo* performance, the findings of this study support the SES-NEG as a promising platform for further topical applications. Its versatility, prolonged skin retention, and limited systemic exposure represent key advantages of this drug delivery system in the context of topical management of skin malignancies

List of Abbreviations

SES: Sesamol

SES-NE- Sesamol Loaded Nanoemulsion

SES-NEG- Sesamol Loaded Nanoemulgel

NE-Nanoemulsion

DLS: Dynamic light scattering

DSC: Differential scanning calorimetry

EE: Entrapment efficiency

NMSC: Non-melanoma skin cancer

PBS: Phosphate buffer saline

PDI: Polydispersity index

PDT: Photodynamic therapy

PII: Primary irritation index

SEM: Scanning electron microscopy

References

1. Linos E, Katz KA, Colditz GA (2016). Skin cancer—the importance of prevention. JAMA Intern. Med. 176(10):1435-6.
2. Sung H, Ferlay J, Siegel RL, Laversanne M, Soerjomataram I, Jemal A, Bray F (2021). Global cancer statistics 2020: GLOBOCAN estimates of incidence and mortality worldwide for 36 cancers in 185 countries. CA Cancer J Clin. 71(3):209-49.
3. Sathishkumar K, Chaturvedi M, Das P, Stephen S, Mathur P (2022). Cancer incidence estimates for 2022 & projection for 2025: result from National Cancer Registry Programme, India. Indian J Med Res. 156(4-5):598-607.
4. Panda S (2010). Nonmelanoma skin cancer in India: Current scenario. Indian J Dermatol. 55(4):373-8.
5. Hasan N, Nadaf A, Imran M, Jiba U, Sheikh A, Almalki WH, Almujri SS, Mohammed YH, Kesharwani P, Ahmad FJ (2023). Skin cancer: understanding the journey of transformation from conventional to advanced treatment approaches. Mol Cancer. 22(1):168.
6. Dekker PK, Mishu MD, Youn R, Baker SB (2021). Serial excision for treatment of non-melanoma skin cancer. Plast Reconstr Surg Glob Open. 9(6):e3607.
7. Nasim M, Khan M, Parveen R, Gull A, Khan S, Ali J (2024). Novel paradigm of therapeutic intervention for skin cancer: challenges and opportunities. Future J Pharm Sci. 10(1):112.
8. Dianzani C, Zara GP, Maina G, Pettazzoni P, Pizzimenti S, Rossi F, Gigliotti CL, Ciamporcero ES, Daga M, Barrera G (2014). Drug delivery nanoparticles in skin cancers. Biomed Res Int. 2014:895986.
9. Gupta N, Gupta GD, Singh D (2022). Localized topical drug delivery systems for skin cancer: Current approaches and future prospects. Front Nanotechnol. 4:1006628.
10. Adnan M, Akhter MH, Afzal O, Altamimi AS, Ahmad I, Alossaimi MA, Jaremko M, Emwas AH, Haider T, Haider MF (2023). Exploring nanocarriers as treatment modalities for skin cancer. Molecules. 28(15):5905.
11. Duarte J, Sharma A, Sharifi E, Damiri F, Berrada M, Khan MA, Singh SK, Dua K, Veiga F, Mascarenhas-Melo F, Pires PC (2023). Topical delivery of NEs for skin cancer treatment. Appl Mater Today. 35:102001.

12. Donthi MR, Munnangi SR, Krishna KV, Saha RN, Singhvi G, Dubey SK (2023). Nanoemulgel: a novel nano carrier as a tool for topical drug delivery. Pharmaceutics. 15(1):164.
13. Singh H, Mishra AK, Mohanto S, Kumar A, Mishra A, Amin R, Darwin CR, Emran TB (2024). A recent update on the connection between dietary phytochemicals and skin cancer: emerging understanding of the molecular mechanism. Ann Med Surg (Lond). 86(10):5877-913.
14. National Center for Biotechnology Information. PubChem Compound Summary for SES (CID 68289). https://pubchem.ncbi.nlm.nih.gov/compound/SES. Accessed Feb. 17, 2026.
15. Geetha T, Rohit B, Pal KI (2009). Sesamol: an efficient antioxidant with potential therapeutic benefits. Med Chem. 5(4):367-71.
16. Nair AB, Dalal P, Kadian V, Kumar S, Kapoor A, Garg M, Rao R, Aldhubiab B, Sreeharsha N, Almuqbil RM, Attimarad M (2022). Formulation, characterization, anti-inflammatory and cytotoxicity study of Sesamol-laden nanosponges. Nanomaterials (Basel). 12(23):4211.
17. Ramachandran S, Rajendra Prasad N, Karthikeyan S (2010). SES inhibits UVB-induced ROS generation and subsequent oxidative damage in cultured human skin dermal fibroblasts. Arch Dermatol Res. 302(10):733-44.
18. Arya H, Mohan C, Pandey S, Verama M, Kumar V (2021). Phytochemical screening of Basella alba leaves extracts and evaluate its efficacy on sun burn (Sun Protection Factor). Eur J Molecular & Clinical Med. 8(1); 417-423.
19. Geetha T, Kapila M, Prakash O, Deol PK, Kakkar V, Kaur IP (2015). Sesamol-loaded solid lipid nanoparticles for treatment of skin cancer. J. Drug Target. 23(2):159-69.
20. Srisongkram T, Weerapreeyakul N, Kärkkäinen J, Rautio J (2019). Role of L-type amino acid transporter 1 (LAT1) for the selective cytotoxicity of Sesamol in human melanoma cells. Molecules. 24(21):3869.
21. Srisongkram T, Weerapreeyakul N. Route of intracellular uptake and cytotoxicity of sesamol, sesamin, and sesamolin in human melanoma SK-MEL-2 cells. Biomedicine & Pharmacotherapy. 2022 Feb 1;146:112528.
22. Gao XJ, Xie GN, Liu L, Fu ZJ, Zhang ZW, Teng LZ (2017). Sesamol attenuates oxidative stress, apoptosis and inflammation in focal cerebral ischemia/reperfusion injury. Exp. Ther. Med. Jul;14(1):841-7.

23. Wu MS, Aquino LB, Barbaza MY, Hsieh CL, De Castro-Cruz KA, Yang LL, Tsai PW (2019). Anti-inflammatory and anticancer properties of bioactive compounds from *Sesamum indicum* L.—A review. Molecules. 24(24):4426.
24. Liu Z, Ren B, Wang Y, Zou C, Qiao Q, Diao Z, Mi Y, Zhu D, Liu X (2017). Sesamol induces human hepatocellular carcinoma cells apoptosis by impairing mitochondrial function and suppressing autophagy. Scientific Reports. 7(1):45728.
25. Jahan S, Sultana N, Ali A, Emad NA, Alam P, Mujeeb M, Aqil M, Ali A (2025). 5-Fluorouracil-and Sesamol-loaded transliposomal gel for skin cancer: in vitro, ex vivo, and dermatokinetic evaluation. ACS Omega. 10(7):6857-75.
26. Geetha T, Singh N, Deol PK, Kaur IP (2015). Biopharmaceutical profiling of Sesamol: physiochemical characterization, gastrointestinal permeability and pharmacokinetic evaluation. RSC Adv. 5(6):4083-91.
27. Geetha T, Kapila M, Prakash O, Deol PK, Kakkar V, Kaur IP (2015). Sesamol-loaded solid lipid nanoparticles for treatment of skin cancer. J Drug Target. 23(2):159-69.
28. Srisongkram T, Bahrami K, Järvinen J, Timonen J, Rautio J, Weerapreeyakul N (2022). Development of SES carbamate-L-phenylalanine prodrug targeting L-Type Amino Acid Transporter1 (LAT1) as a potential antiproliferative agent against melanoma. Int J Mol Sci. 23(15):8446.
29. Prado VC, Moenke K, Pegoraro NS, Saccol CP, Nogueira-Librelotto DR, Rechia GC, Oliveira SM, Cruz L (2025). Nano-based hydrogel for cutaneous SES delivery in uvb-induced skin injury. AAPS PharmSciTech. 26(3):75.
30. Sghier K, Mur M, Veiga F, Paiva-Santos AC, Pires PC (2024). Novel therapeutic hybrid systems using hydrogels and nanotechnology: a focus on nanoemulgels for the treatment of skin diseases. Gels. 10(1):45.
31. Chellapa P, Mohamed AT, Keleb EI, Elmahgoubi A, Eid AM, Issa YS, Elmarzugi NA (2015). NE and nanoemulgel as a topical formulation. IOSR J Pharm. 5(10):43-7.
32. DeLuca AM, Srinivas A, Alani RM. BRAF kinase in melanoma development and progression. Expert reviews in molecular medicine. 2008 Feb;10:e6.
33. Pettersen EF, Goddard TD, Huang CC, Couch GS, Greenblatt DM, Meng EC, Ferrin TE. **UCSF Chimera—A visualization system for exploratory research and analysis.** *Journal of Computational Chemistry.* 2004;25(13):1605–1612. doi:10.1002/jcc.20084.
34. Advanced Chemistry Development, Inc. ACD/ChemSketch, Version 2025.2.5. Toronto (ON), Canada: ACD/Labs; 2025 (www.acdlabs.com).

35. Thakur Aman, Paliwal D, Mehta V, Singh PR. PharmoDock: A User-Friendly Molecular Docking Platform for Structure-Based Drug Design and Virtual Screening. Zenodo; 2026 (https://zenodo.org/records/19522194).
36. Thakur Aman, Paliwal D, Mehta V, Singh PR. PharmoADMET: An Integrated Open-Source Platform for In Silico ADMET Prediction and Analysis. Zenodo; 2026 (https://zenodo.org/records/19648345).
37. Paliwal D, Mondal R, Thakur A. 2D-QSAR and molecular docking based virtual screening and molecular dynamic simulation of the indole based herbal molecules for the discovery of potent molecules in the treatment of Alzheimer's disease. In Silico Pharmacology. 2025 Jun 7;13(2):81.
38. Singh N, Kushwaha P, Gupta A, Ved A, Swarup S (2022). Development and evaluation of SES-loaded self nanoemulsifying drug delivery system for breast cancer. Pharmacogn Mag. 18(77):94-102.
39. Bhargav E, Chaithanya Barghav G, Padmanabha Reddy Y, Pavan kumar C, Ramalingam P, Haranath C (2020). A Design of Experiment (DoE) based approach for development and optimization of nanosuspensions of telmisartan, a BCS class II antihypertensive drug. Future J Pharm Sci. 6(1):14.
40. Koh JK, Lai CW, Wong JP (2026). Microemulsions and NEs for cosmetic applications. In Nanotechnology in Cosmeceuticals. Academic Press.189-215.
41. Nagaraja S, Basavarajappa GM, Attimarad M, Pund S (2021). Topical nanoemulgel for the treatment of skin cancer: Proof-of-technology. Pharmaceutics. 13(6):902.
42. Prado VC, Moenke K, Osmari BF, Pegoraro NS, Oliveira SM, Cruz L (2023). Development of guar gum hydrogel containing SES-loaded nanocapsules designed for irritant contact dermatitis treatment induced by croton oil application. Pharmaceutics. 15(1):285.
43. Pont I, Felipe R, Frías JC, Chicote JU, García-España A, García-España E, Albelda MT (2024). An effective liposome-based nanodelivery system for naphthalene derivative polyamines with antitumor activity. Biomolecules. 14(11):1347.
44. Yadav R, Sanduja M, Kumar V, Sharma K, Khan S, Kumar K (2024). Microwave-assisted synthetic pathways of pyrrole: a comprehensive review. Asian J Organic Chemistry. 13(12); e202400401.
45. Gómez-Lázaro L, Martín-Sabroso C, Aparicio-Blanco J, Torres-Suárez AI (2024). Assessment of in vitro release testing methods for colloidal drug carriers: the lack of standardized protocols. Pharmaceutics. 16(1):103.

46. Ribeiro BC, Cintra ER, Lima EM, Silva LA, Diniz DG (2023). Evaluation of testosterone compatibility with different excipients for the development of a self-emulsifying drug delivery system. J Therm Anal Calorim. 148(1):159-68.
47. Chitkara A, Mangla B, Kumar P, Javed S, Ahsan W, Popli H (2022). Design-of-experiments (DoE)-assisted fabrication of quercetin-loaded nanoemulgel and its evaluation against human skin cancer cell lines Pharmaceutics. 14(11):2517.
48. Bahloul B, Ben Bnina E, Dridi D, Bouhamed A, Castillo Henríquez L, Flamini G, Vega-Baudrit JR (2024). Development and investigation of a nanoemulgel formulated from *Tunisian Opuntia ficus*-indica L. seed oil for enhanced wound healing activity. Gels. 10(9):582.
49. Alhasso B, Ghori MU, Rout SP, Conway BR (2023). Development of a nanoemulgel for the topical application of mupirocin. Pharmaceutics. 15(10):2387.
50. Tiwari R, Sethi P, Rudrangi S. R. S, Padarthi P K, Kumar V, Rudrangi S, Vaghela K (2024). Inulin: a multifaceted ingredient in pharmaceutical sciences. J Biomaterials Sci, Polymer Edition.. 35(16); 2570-2595.
51. Ullah N, Amin A, Farid A, Selim S, Rashid SA, Aziz MI, Kamran SH, Khan MA, Rahim Khan N, Mashal S, Mohtasheemul Hasan M (2023). Development and evaluation of essential oil-based nanoemulgel formulation for the treatment of oral bacterial infections. Gels. 9(3):252.
52. Kolle SN, Teubner W, Landsiedel R (2017). Modern skin toxicity testing strategies. In Environment and Skin. Cham: Springer. 27-40.
53. Khan R, Mirza MA, Aqil M, Alex TS, Raj N, Manzoor N, Naseef PP, Saheer Kuruniyan M, Iqbal Z (2023). *In vitro* and *in vivo* investigation of a dual-targeted NE gel for the amelioration of psoriasis. Gels. 9(2):112.
54. Shaker DS, Ishak RA, Ghoneim A, Elhuoni MA (2019). NE: A review on mechanisms for the transdermal delivery of hydrophobic and hydrophilic drugs. Sci Pharm. 87(3):17.
55. Kumar S, Wadhwa K, Pahwa R, Ali J, Baboota S (2024). Screening of surfactant mixture ratio for preparation of oil-in-water NE: A technical note. J Appl Pharm Sci. 14(10):121-7.
56. Koushik Y, Rama Rao N, Sri Venkatesh U, Rami Reddy GV, Surendra AV, Sreenu T (2025). Formulation and optimization of a *Melissa officinalis*-loaded nanoemulgel for anti-inflammatory therapy using Design of Experiments (DoE). Gels. 11(10):776.
57. Kumar N, Kumar V, Chowdhary Y (2022). A review on synthesis methods of tricyclic 1, 2, 3, 4-tetrahydrocarbazoles. World J Advanced Res and Reviews.. 13(1); 160-171.

58. Tamboli AM, Tade JM (2025). Zeta potential: a comprehensive review. Int Res J Pharm Med Sci. 8(2):115-24.
59. Singh N, Khullar N, Kakkar V, Kaur IP (2015). Sesamol loaded solid lipid nanoparticles: a promising intervention for control of carbon tetrachloride induced hepatotoxicity. BMC Complement Altern Med. 15(1):142.
60. Jadhav ST, Salunkhe VR, Bhinge SD (2023). NE drug delivery system loaded with imiquimod: a QbD-based strategy for augmenting anti-cancer effects. Future J Pharm Sci. 9(1):120.
61. Klang V, Matsko NB, Valenta C, Hofer F (2012). Electron microscopy of NEs: An essential tool for characterisation and stability assessment. Micron. 43(2-3):85-103.
62. Farooq U, Rasul A, Zafarullah M, Abbas G, Rasool M, Ali F, Ahmed S, Javaid Z, Abid Z, Riaz H, Mahmood Arshad RK (2021). NEs as novel nanocarrieres for drug delivery across the skin: *In-vitro, in-vivo* evaluation of miconazole NEs for treatment of Candidiasis albicans. Des Monomers Polym. 24(1):240-58.
63. Jain Y, Jain G, Dutta D, Yadav M (2025). Transferosomes as a promising platform for targeted antifungal drug delivery. Current Fungal Infection Reports. 19:16;1-16.
64. Lukić M, Pantelić I, Savić SD (2021). Towards optimal ph of the skin and topical formulations: From the current state of the art to tailored products. Cosmetics. 8(3):69.
65. Sandhir V, Kumar V, Kumar V (2021). Prognosticating the spread of COVID-19 pandemic based on optimal ARIMA estimators. Endocrine, Metabolic & Immune Disorders-Drug Targets. 21(4); 586-591.
66. Zafar A, Yasir M, Mujtaba MA, Khalid M, Panda DS, Singh L, Alsaidan OA, Quazi AM (2025). Development of SES loaded-polymer-lipid blend nanoparticles: statistical optimization, in-vitro, and preclinical assessment. J Pharm Innov. 20(4):119.
67. Fajrin FA, Holidah D, Christianty FM, Dewi IP, Espanola BF, Parastuti DP, Fahrudin MN, Imamah N, Widiyatno WP (2025). Acute dermal toxicity test and anti-inflammatory activity of emulgel from cocoa pod husk (*Theobroma Cacao* l.) ethanol extract. Phytomedicine Plus. 100899.
68. Latif MS, Nawaz A, Asmari M, Uddin J, Ullah H, Ahmad S (2022). Formulation development and in vitro/in vivo characterization of methotrexate-loaded NE gel formulations for enhanced topical delivery. Gels. 9(1):3.
69. Guo W, Wang H, Li C. Signal pathways of melanoma and targeted therapy. Signal transduction and targeted therapy. 2021 Dec 20;6(1):424.

70. Nawrot-Hadzik I, Choromańska A, Abel R, Preissner R, Saczko J, Matkowski A, Hadzik J. Cytotoxic effect of vanicosides A and B from Reynoutria sachalinensis against melanotic and amelanotic melanoma cell lines and in silico evaluation for inhibition of BRAFV600E and MEK1. International Journal of Molecular Sciences. 2020 Jun 29;21(13):4611.
71. Wu XL, Liou CJ, Li ZY, Lai XY, Fang LW, Huang WC. Sesamol suppresses the inflammatory response by inhibiting NF-κB/MAPK activation and upregulating AMP kinase signaling in RAW 264.7 macrophages. Inflammation Research. 2015 Aug;64(8):577-88.
72. Kumar G, Virmani T, Pathak K, Kamaly OA, Saleh A. Central composite design implemented azilsartan medoxomil loaded nanoemulsion to improve its aqueous solubility and intestinal permeability: in vitro and ex vivo evaluation. Pharmaceuticals. 2022 Oct 29;15(11):1343.
73. Singh D, Garg G, Gupta R. Design and characterization of wheatgrass extract Nanoemulsion-Based hydrogel for enhanced dermal targeting in skin cancer. Applied Nanoscience. 2026 Apr;16(2):16.
74. Lei T, Srinivasan S, Tang Y, Manchanda R, Nagesetti A, Fernandez-Fernandez A, McGoron AJ. Comparing cellular uptake and cytotoxicity of targeted drug carriers in cancer cell lines with different drug resistance mechanisms. Nanomedicine: Nanotechnology, Biology and Medicine. 2011 Jun 1;7(3):324-32.